



Tracking rockglacier evolution in the Eastern Alps from the Lateglacial to the early Holocene

Olivia Steinemann^{a,*}, Jürgen M. Reitner^b, Susan Ivy-Ochs^a, Marcus Christl^a, Hans-Arno Synal^a

^a Laboratory of Ion Beam Physics, ETH Zürich, Otto-Stern-Weg 5, 8093, Zürich, Switzerland

^b Geological Survey of Austria, Neulinggasse 38, 1030, Vienna, Austria

ARTICLE INFO

Article history:

Received 21 February 2020

Received in revised form

2 June 2020

Accepted 9 June 2020

Available online 7 July 2020

Keywords:

Cosmogenic ¹⁰Be

Permafrost development

Relict rockglaciers

Periglacial

Glacier-rockglacier interaction

Gschnitz stadial

Carinthia

ABSTRACT

Relict rockglaciers are distinctive indicators of past permafrost occurrence. Their lower limit is attributed to a former mean annual air temperature (MAAT) of below $-2\text{ }^{\circ}\text{C}$. This study provides a comprehensive dataset of 34 ¹⁰Be exposure ages from boulders along two complex series of relict rockglaciers, called Tandl rockglaciers and Norbert rockglaciers (Carinthia, Austria). The lowest Tandl rockglacier complex stabilised around 14 ka at an elevation of 1350 m a.s.l., the lowest Norbert rockglaciers (1580 and 1730 m a.s.l.) stabilised around 15.7 ka. Additionally, in both study sites the low elevation relict rockglaciers interacted with glacial deposits of the local pre-Bølling glaciers (Gschnitz stadial glacier). Temperature lowering based on our data of the Gschnitz rockglaciers ranges between 6.3 and 4.5 $^{\circ}\text{C}$ compared to modern MAAT. The cross-cutting relationships of the rockglaciers and the glacial deposits together with the exposure ages of the rockglaciers, indicate that these rockglaciers, and therewith also permafrost, developed shortly after or even simultaneously with retreat of the Gschnitz stadial glaciers. This is the first permafrost formation in the Alpine areas after the retreat of the (warm-based) Last Glacial Maximum glaciers. The Tandl and Norbert rockglacier lobes located at higher elevations, up to about 2300 m a.s.l., finally stabilised in the early Holocene; ages of several dated lobes lie between 12–10 ka. At this time, which corresponds to the Egesen stadial (Younger Dryas) cold phase, rockglaciers and glaciers co-existed. From the lowest position of the Egesen rockglacier lobe at the Tandl site (1700 m a.s.l.), a temperature lowering for the Egesen stadial of $-4.6\text{ }^{\circ}\text{C}$ was calculated. This study highlights the potential of relict rockglacier deposits as an independent paleoclimate archive and their usefulness for reconstruction of past permafrost development and distribution in high mountain areas when they can be placed in a temporal framework.

© 2020 Elsevier Ltd. All rights reserved.

1. Introduction

Rockglaciers are among the most striking and immediately recognisable periglacial landforms in high mountain areas (Haeberli, 1985; Barsch, 1996; Kääh, 2013; Ballantyne, 2018; Jones et al., 2019). They stand tens of meters above the surrounding terrain with their steep ($>35^{\circ}$) front and side walls. Barsch (1996) defined rockglaciers as "... lobate or tongue-shaped bodies of perennially frozen unconsolidated material supersaturated with

interstitial ice and ice lenses that move downslope or downvalley by creep as a consequence of the deformation of ice contained in them and which are, thus, features of cohesive flow". The surface relief is generally blocky and indicative of the creeping processes. It is often characterized by transverse furrows and ridges in the lower and flow-parallel ridges in the upper part (Haeberli, 1985; Ikeda and Matsuoka, 2002; Frehner et al., 2015).

Active rockglaciers occur within the local permafrost belt and if they are not hindered by topography, the front of the rockglacier corresponds to the lower limit of discontinuous permafrost, indicating a mean annual air temperature (MAAT) of $< -2\text{ }^{\circ}\text{C}$ (Haeberli, 1985; Barsch, 1996). Cold but rather dry climatic conditions and a lithology that constantly provides abundant blocky debris (e.g. granite, gneiss, massive limestone) favour formation and persistence of active rockglaciers (Frauenfelder, 2003; Haeberli et al.,

* Corresponding author.

E-mail addresses: okronig@phys.ethz.ch (O. Steinemann), juergen.reitner@geologie.ac.at (J.M. Reitner), ivy@phys.ethz.ch (S. Ivy-Ochs), mchristl@phys.ethz.ch (M. Christl), synalha@phys.ethz.ch (H.-A. Synal).

2006; Kenner and Magnusson, 2017). Depending on various influences such as climate (MAAT, mean annual precipitation (MAP), wind sheltering), topography, aspect, and lithology, a variety of forms are possible, from very simple rockglaciers to highly complex ones with overlapping lobes (Brazier et al., 1998; Gruber and Hoelzle, 2001; Dramis et al., 2003; Johnson et al., 2007; Kenner and Magnusson, 2017). In the Alps rates of movement range in the order of centimetres to few meters per year with average values around 0.2–0.5 m/a (Kääb et al., 2003, 2007; Frauenfelder et al., 2004; Delaloye et al., 2010). Within the last few years a general trend in rockglacier acceleration has been observed (Roer et al., 2005; Delaloye et al., 2013; Bodin et al., 2017; Eriksen et al., 2018), which is correlated to increasing air temperatures. A warming climate leads to rise of the permafrost limit to higher elevations and as a consequence the internal ice of rockglaciers starts to melt. As soon as the ice content has shrunk below a critical volume required for movement, the rockglacier stabilises and becomes climatically inactive. In the moment of complete loss of the interstitial ice, it turns from an inactive into a relict rockglacier, which is geomorphologically characterized by deep depressions and collapse features due to the ice loss, but retains most of its morphology (Barsch, 1996). At that moment, blocks that may have been shifting or rotating gain a stable position.

One of the first researchers to write down thoughts on rockglacier formation and formation age was Capps (1910). He links their formation to a post-glacial environment, arguing that rockglacier formation starts after deglaciation, when areas became ice-free and permafrost development starts. For the Eastern Alps, this began at around 19–18 ka when glaciers of the Last Glacial Maximum (LGM) network of transection glaciers (Van Husen, 1987) receded back from the forelands (Reitner, 2007a; Ivy-Ochs, 2015; Monegato et al., 2017). Associated ice surface lowering in the high Alps has been dated to 19–18 ka (Wirsig et al., 2016). In most areas LGM glaciers were warm-based as shown by the presence of abundant glacial erosional features and the facies of subglacial sediments (Menzies and Reitner, 2016). During the Oldest Dryas (18–14.6 ka), glacier variations are referred to the early Lateglacial phase of ice decay (Reitner, 2007a) and the Gschnitz stadial (17–16 ka) (Ivy-Ochs et al., 2006a; Reitner et al., 2016). This is followed by the Bølling-Allerød interstadial (14.7–12.9 ka) (Walker et al., 1999), and the Egesen stadial, with glaciers responding to the Younger Dryas cold phase (12.9–11.7 ka) (Kerschner, 1980; Ivy-Ochs et al., 1996, 2009; Cossart et al., 2012; Bichler et al., 2016; Drescher-Schneider and Reitner, 2018; Scotti and Brardinoni, 2018). In contrast to the Lateglacial glacier fluctuation history, almost nothing is known about the onset of permafrost in the formerly glaciated areas in the Alps after the LGM and its further chronology of expansion and recession.

As relict rockglaciers initially formed under permafrost conditions, their position gives direct evidence of the lower limit of permafrost at the time of their activity (Barsch, 1996). This relationship between active rockglaciers and climate makes relict rockglaciers attractive for constraining past MAAT (Kellerer-Pirklbauer and Kaufmann, 2012; Moran et al., 2016). The potential of relict rockglaciers for constraining past climate conditions was already recognized in the early days of rockglacier research (Kerschner, 1978, 1983; 1985; Barsch, 1992). However, at that time it was not possible to absolutely date them, which is essential to draw conclusions about the past. Knowing the age of a rockglacier, its moment of inception or decline into inactivity, has been and remains difficult to constrain. Periods of rockglacier activity may be estimated through cross-cutting relationships of rockglaciers with glacial landforms (Kerschner, 1978; Sailer and Kerschner, 1999). In addition to using rockglacier-glacier interactions to gain a relative age for a rockglacier, several other indirect methods exist. For

example, radiocarbon dating of organic material found within or below a rockglacier (Haeberli et al., 1999; Scapozza et al., 2010; Krainer et al., 2015), Schmidt-hammer and weathering rind thickness measurements on boulders (Frauenfelder et al., 2004; Böhlert et al., 2011a, 2011b) or luminescence methods (Fuchs et al., 2013) can be applied. Lately, it has been shown that absolute ages of relict rockglaciers or related periglacial landforms can be determined by applying cosmogenic nuclide exposure dating directly on boulders of the deposit (Barrows et al., 2004; Ballantyne et al., 2009; Hippolyte et al., 2009; Ivy-Ochs et al., 2009; Moran et al., 2016; Palacios et al., 2016; Andrés et al., 2018). But it is somewhat controversial due to problems of ambivalent interpretation, including concerns about inheritance and the length of time required for final rockglacier stabilisation.

The goals of this study are to investigate two geomorphologically well-defined rockglacier systems in the Eastern Alps (Fig. 1). Rockglacier deposits in each system are located at rather low elevations suggesting they are older than many other rockglacier deposits in the region or in the Alps. Notably, the two sites are located relatively close to each other (<10 km) and have different aspects one facing northeast and the other southwest. A primary aim is to examine the applicability of rockglacier deposits as paleoclimate archives, which is only possible if they can be placed in a chronological framework. Cosmogenic nuclides are a suitable tool, as boulders in the deposit can be directly dated. In this study numerous boulders in a sequence of related rockglacier lobes were dated and the results were scrutinized in light of field relationships, providing insights into not only periods of activity but also the morphodynamic development of the rockglacier complexes over time. As even the oldest rockglaciers we studied appear to have advanced into recently ice-free terrain, this gives us the opportunity to examine glacier-rockglacier interactions throughout the Lateglacial and early Holocene. Additionally, our data from each of these archives allows inferences to be made on paleoclimatic parameters.

2. Study sites

In the Reisseck group (a part of the Hohe Tauern mountain range) located in the Eastern Alps (Fig. 1), in the province of Carinthia, Austria, two outstanding series of complex, multi-lobed, talus-derived (Barsch, 1996) relict rockglaciers can be found (Reitner, 2007b; Kellerer-Pirklbauer et al., 2012). These are the Tandl rockglaciers (46° 56.99' N, 13° 26.04' E) and the Norbert rockglaciers (46° 54.26' N, 13° 22.86' E). They span in elevation from 1220 m a.s.l. at Tandl and 1580 m a.s.l. at Norbert and up to approximately 2300 m a.s.l. The Tandl rockglaciers are located in a tributary valley on the western side of the Malta Valley (829 m a.s.l.). The Norbert rockglaciers (named after the local alp) are located in a northern tributary valley of the Möll Valley (589 m a.s.l.). According to the permafrost map (Boeckli et al., 2012b, 2012a) and the elevation of the -2°C isotherm at around 2600 m a.s.l., there is presently no permafrost at the study sites. However, the highest mountain peaks may still contain permafrost (Hochkedl 2558 m a.s.l., Sonnblick 2515 m a.s.l., Tandelspitze 2633 m a.s.l.). The two valleys receive between 1000 and 1750 h of sunshine over the year (Fig. 2), annual precipitation of 1250–1750 mm and around 0.75–2 m snow during the winter (Data source: data.gv.at, Land Kärnten, accessed April 2019). MAAT and mean annual summer temperatures (JJA) were retrieved from data series of the Zentralanstalt für Meteorologie und Geodynamik (Central Office for Meteorology and Geodynamics). They were developed for the Hohe Tauern region (ca. 40 km distance to the study sites) in the course of the project “A tale of two valleys” (<http://www.zamg.ac.at/a-tale-of-two-valleys>, (Auer et al., 2010)) and are available for altitudes

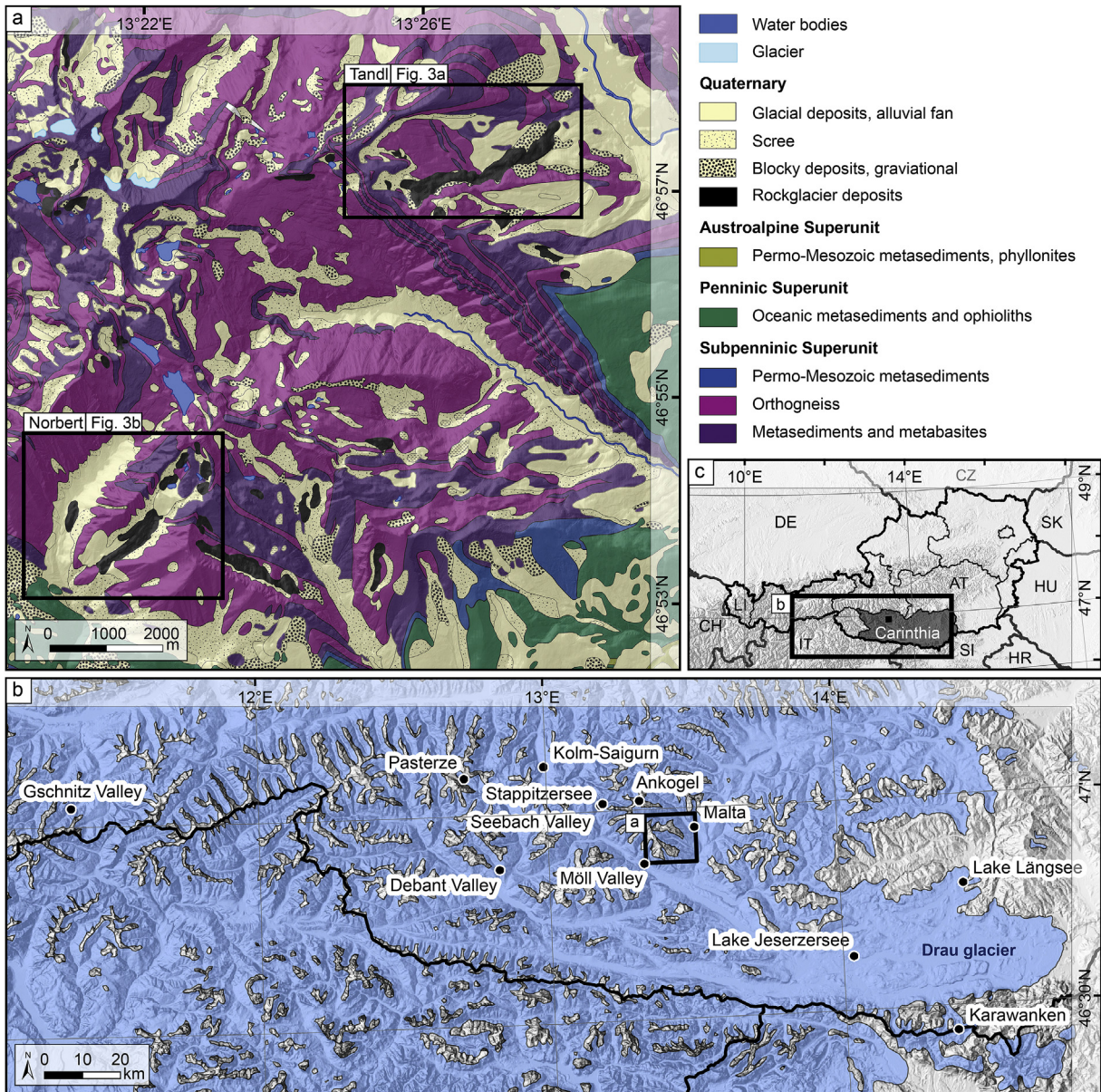


Fig. 1. Geological and overview maps of the study area. (a) Geological map of the main units of the Reisseck group region modified from Pestal et al. (2006). The two study sites are indicated by black rectangles. (b) Overview map of Carinthia, showing locations discussed in text, black rectangle shows extent of (a). Last Glacial Maximum ice extent taken from Ehlers and Gibbard (2004). (c) Overview map of Austria, with the province Carinthia highlighted in grey. The big black rectangle shows extent of (b), the small black square the extent of (a). (For interpretation of the references to color in this figure legend, the reader is referred to the Web version of this article.)

of 3100 m a.s.l. (Hoher Sonnblick), 2500 m a.s.l., 2000 m a.s.l. and 1500 m a.s.l. We use the 20th century mean (1901–2000) as a reference (“modern”) for all calculations.

Geologically, both study sites are located in the Venediger nappe system, which is part of the Subpenninic superunit of the Tauern Window (Fig. 1a) (Schuster et al., 2006). The dominant lithologies in the areas are augen and banded gneiss (Granitoide des Hochalmkerns), and biotite granite gneiss (Granitoide des Gössaukerns), both also known as Zentralgneiss (shown as orthogneiss in Fig. 1a) (Pestal et al., 2006). During the LGM this area was covered by the Drau Glacier system (Fig. 1b) (Van Husen, 1987; Ehlers et al., 2011).

3. Methods

3.1. Fieldwork

Periglacial and glacial landforms were identified and mapped during two field campaigns (2015, 2016) utilizing and improving the map of Pestal et al. (2006). Detailed sedimentological analysis of landforms was applied to distinguish relict rockglaciers from landslide, glacial and debris-covered glacier deposits. Field mapping was augmented by landform interpretation based on topographic and hillshade maps. For creating the final geomorphological map, collected field information was digitized in Arc-GIS (ESRI Inc.) and completed with a 1 m resolution digital

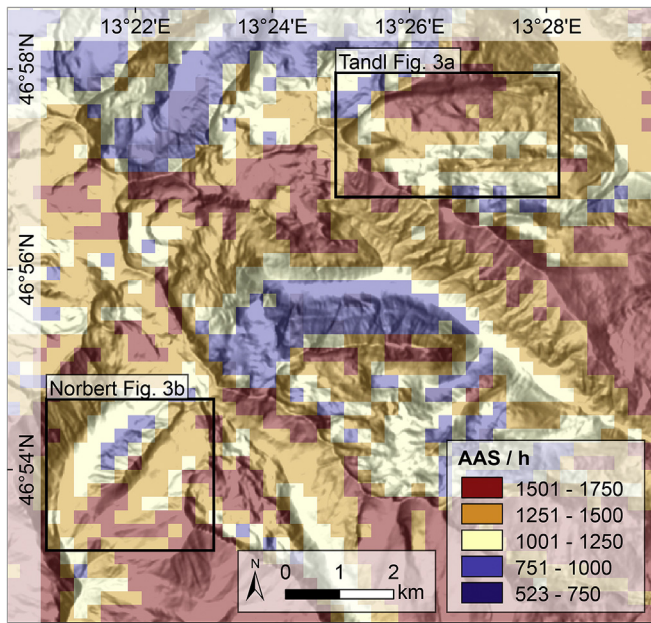


Fig. 2. Absolute annual sunshine duration (AAS) map of the Reisseck group region. Size and extent corresponds to Fig. 1a. Study sites are shown as black rectangle. Data source: data.gv.at, Land Kärnten, accessed April 2019. (For interpretation of the references to color in this figure legend, the reader is referred to the Web version of this article.)

elevation model (DEM; provided by the province of Carinthia) that allowed further surface analysis (e.g. slope and aspect maps).

3.2. Paleo-glacier reconstruction and paleo-ELA calculation

Field observations suggested that the Tandl site was covered by a glacier prior to rockglacier formation. Hence, the position of the paleo-ELA (equilibrium line altitude) could provide more details for constraining rockglacier evolution and rockglacier-glacier interactions. To reconstruct the paleo-glacier extent and calculate its paleo-ELA, the ArcGIS toolbox GlaRE and a related ELA toolbox were used (Pellitero et al., 2015, 2016). The former calculates an ice thickness from the bed topography, based on glacier physics and ice dynamics. As input, a paleo-surface-DEM is needed, as the glacier to be reconstructed existed before the rockglaciers evolved. All relict rockglacier deposits were removed from the present-day landscape by adjusting contour lines (20 m interval), which were calculated from the original DEM, to approximately fit the topography adjacent to the rockglacier deposits. From the new isohypses, a paleo-DEM (without rockglacier deposits) was generated. Further, realistic values for basal shear stress were implemented according to the slope of the topography (Pellitero et al., 2016): 110 kPa for the less steep upper half, and 160 kPa for the lower and steeper part of the valley.

The second toolbox uses empirically determined mathematical relationships to calculate the paleo-ELA of the reconstructed glacier (Ohmura et al., 1992; Kerschner et al., 2000; González Trueba and Serrano Cañadas, 2004; Benn and Hulton, 2010; Pellitero et al., 2015). For the Tandl paleo-ELA estimation the accumulation area to the total area ratio (AAR) method was used, implementing ratios of 0.6 and 0.65, common values suggested in literature (Gross et al., 1977; Bakke and Nesje, 2011).

3.3. Image correlation

ImGraft (v2.0.2), an open-source MATLAB toolbox for image

correlation (Messerli and Grinsted, 2015), was used to examine if the highest rockglaciers of the Tandl area are still moving. Because of their morphology, elevation and aspect it could be possible that they are still active or intact. On the basis of two orthophotos with the same spatial resolution but from different years (2003 and 2013), the templatematch code tracks displacements between the image pair and shows as a result the horizontal movement between the two orthophotos (Data source: data.gv.at, Land Kärnten, accessed April 2019).

3.4. ^{10}Be exposure dating

3.4.1. Sampling

To date the relict rockglacier lobes, 34 samples were taken for ^{10}Be analysis. The largest (1–7 m size) and well exposed boulders (compared to their neighbouring boulders) of quartz-rich lithologies (gneiss and quartz veins) with, horizontal, unplucked but weathered surfaces were selected for sampling. Boulders located at the frontal crest of the rockglacier lobe or from transverse ridges were preferred, as this position is thought to be most stable and diminishes the possibility of post-depositional toppling due to ice loss. The upper 1–4 cm of each boulder were taken with an angle grinder, hammer and chisel. Topographic shielding, strike and dip of the sampled surface were measured.

3.4.2. Sample preparation, AMS measurement and exposure age calculation

Tables 1 and 2 summarise the main sample information, measured ^{10}Be concentrations and calculated exposure ages. Samples were processed in laboratories at the ETH Zürich (Laboratory of Ion Beam Physics), following the methods of Kohl and Nishiizumi (1992) and Ivy-Ochs et al. (2006b) with some minor adaptations. The crushed and sieved (<800 μm) samples were cleaned with a weak HF solution (10%) to isolate pure quartz. A weighted amount of 0.250 mg ^9Be carrier solution was added to each sample. Chemical isolation of the beryllium was achieved using two ion exchange columns followed by $\text{Be}(\text{OH})_2$ precipitation. The final precipitates were oxidized and pressed into targets. $^{10}\text{Be}/^9\text{Be}$ ratio measurements were performed at the Laboratory of Ion Beam Physics at the ETH Zürich on the 600 kV Tandy AMS facility (Christl et al., 2013) relative to the 07KNSTD standard (Nishiizumi et al., 2007). Exposure age calculations were accomplished with the CRONUS-Earth online exposure age calculator (Balco et al., 2008) using the scaling model of Lal (1991)/Stone (2000) and the north-eastern North America ^{10}Be production rate of 3.87 ± 0.19 at/g/a, which is consistent with the local production rate determined by Claude et al. (2014) in the southern Swiss Alps. To obtain lower uncertainties, three samples were repeated (Tandl3, Tandl4, Tandl5). The exposure ages of the redone samples agree well with the previous ones, but with clearly smaller uncertainties. Hence, the given exposure ages of those three samples are the weighted mean of both results and are marked with the superscript “wm” in Table 1. No correction for snow cover was applied. Snow cover of 50 cm during 6 months a year would increase the exposure ages by approximately 6% (cf. Delunel et al., 2014). An erosion rate of 1 mm/ka (André, 2002) was used to correct for boulder surface weathering. Erosion-corrected ages are used for further discussion below and are shown on the geomorphological maps of the Tandl site (Fig. 3a) and the Norbert site (Fig. 3b).

4. Results and interpretation: morphological evolution of the Reisseck group rockglaciers

The obtained exposure ages range from 4.1 (± 0.3) ka to 15.7

Table 1

Sample information of the Tandl site. Summarising location and sample information, blank corrected AMS concentrations and calculated exposure ages. Given errors are at the 1σ level including analytical uncertainties, and external uncertainties in parenthesis.

Sample name	Landform	Latitude	Longitude	Elevation	Thickness	Shielding correction ^a	$^{10}\text{Be}^b \times 10^4$	Exposure age ^c	Exposure age ^c , erosion corrected ^d
		DD	DD	m	cm		at/g	kyr	kyr
Tan1	TA3	46.957	13.461	1463	3	0.9650	18.34±0.62	14.2±0.5(0.8)	14.4±0.5 (0.9)
Tan2	TA3	46.956	13.460	1475	2	0.9680	18.24±1.11	13.9±0.9(1.1)	14.0±0.9 (1.1)
Tandl3 ^{wm}	TA1	46.960	13.463	1291	3	0.9840	15.84±1.30	13.6±0.6 (0.9)	13.8±0.7 (0.9)
Tandl4 ^{wm}	TA1	46.960	13.463	1296	2	0.9679	15.73±2.16	13.6±0.6 (0.9)	13.7±0.7 (0.9)
Tandl5 ^{wm}	TA1	46.960	13.463	1310	3	0.9530	16.88±2.67	15.5±0.7 (1.0)	15.7±0.7 (1.1)
Tandl6	TB1	46.955	13.453	1735	2	0.9831	19.34±0.99	12.0±0.6 (0.9)	12.1±0.6 (0.9)
Tandl7	TB1	46.955	13.452	1737	2	0.9720	18.20±1.01	11.3±0.6 (0.8)	11.4±0.6 (0.8)
Tandl8	TB1	46.954	13.453	1756	2	0.9803	16.91±0.90	10.3±0.5 (0.7)	10.3±0.6 (0.8)
Tandl9*	TB1	46.954	13.453	1756	1	0.9501	17.10±0.84	10.8±0.5 (0.8)	10.9±0.5 (0.8)
Tandl10*	TB1	46.954	13.454	1725	1	0.9802	19.02±0.88	11.9±0.6 (0.8)	12.0±0.6 (0.8)
Tandl11*	TB1	46.955	13.454	1704	1	0.9729	14.58±0.82	9.2±0.5 (0.7)	9.2±0.5 (0.7)
Tandl12*	TA5	46.956	13.455	1667	1	0.9651	21.56±1.07	14.2±0.7 (1.0)	14.3±0.7 (1.0)
Tandl13*	TA4	46.958	13.458	1529	3	0.9574	16.88±1.02	12.8±0.8 (1.0)	13.0±0.8 (1.0)
Tandl14*	moraine	46.950	13.425	2332	1	0.9544	23.02±1.20	9.4±0.5 (0.7)	9.5±0.5 (0.7)
Tandl15	TC4	46.949	13.431	2289	2	0.9718	22.06±0.77	9.3±0.3 (0.6)	9.4±0.3 (0.6)
Tandl16	TC4	46.949	13.431	2296	1.5	0.9495	22.36±0.68	9.5±0.3 (0.5)	9.5±0.3 (0.6)
Tandl17*	TC3	46.950	13.435	2181	2.5	0.9759	18.39±1.63	8.3±0.7 (0.8)	8.4±0.8 (0.9)
Tandl18	TC3	46.950	13.435	2184	2	0.9759	16.74±0.78	7.5±0.4 (0.5)	7.5±0.4 (0.5)
Tandl19	TC1	46.952	13.444	1971	1	0.9685	16.11±0.57	8.4±0.3 (0.5)	8.4±0.3 (0.5)
Tandl20*	TC1	46.952	13.444	1972	1	0.9759	7.93±0.52	4.1±0.3 (0.3)	4.1±0.3 (0.3)

^a Shielding correction includes the topographic shielding due to surrounding landscape and the dip of the sampled surface.

^b AMS measurement errors are at the 1σ level. Sample ratios are normalized to the 07KNSTD standard.

^c Age errors are internal errors. External errors are given in parentheses.

^d Exposure ages have been corrected for a surface erosion rate of 1 mm ka^{-1}

* Blank correction value of $^{10}\text{Be}/^9\text{Be} = (6.62 \pm 1.37) \times 10^{-15}$, for the other samples a long-term laboratory blank of $^{10}\text{Be}/^9\text{Be} = (3.67 \pm 2.17) \times 10^{-15}$ was used.

^{wm} Exposure ages are weighted mean of two samples.

Table 2

Sample information of the Norbert site. Summarising location and sample information, blank corrected AMS concentrations and calculated exposure ages. Given errors are at the 1σ level including analytical uncertainties, and external uncertainties in parenthesis.

Sample name	Landform	Latitude	Longitude	Elevation	Thick-ness	Shielding correction ^a	$^{10}\text{Be}^b \times 10^4$	Exposure age ^c	Exposure age ^c , erosion corrected ^d
		DD	DD	m	cm		at/g	kyr	kyr
Norb1	d-c. glacier	46.889	13.357	1709	1.5	0.9890	25.47±1.42	15.8±0.9 (1.2)	16.0±0.9 (1.2)
Norb2	d-c. glacier	46.889	13.358	1713	1	0.9682	23.41±1.51	14.8±1.0 (1.2)	15.0±1.0 (1.2)
Norb3	d-c. glacier	46.889	13.358	1706	1	0.9878	25.36±1.05	15.8±0.7 (1.0)	16.0±0.7 (1.0)
Norb4	d-c. glacier	46.890	13.357	1712	2	0.9869	25.49±0.94	15.9±0.6 (1.0)	16.1±0.6 (1.0)
Norb5	NA2	46.891	13.360	1741	3	0.9879	26.70±1.42	16.4±0.9 (1.2)	16.7±0.9 (1.2)
Norb6	NA2	46.891	13.360	1746	1.5	0.9553	24.83±0.97	15.5±0.6 (1.0)	15.7±0.6 (1.0)
Norb7	NA2	46.891	13.360	1746	1	0.9712	25.11±1.85	15.5±1.2 (1.4)	15.7±1.2 (1.4)
Norb8	NA1	46.897	13.350	1598	2	0.9498	20.47±1.71	14.5±1.2 (1.4)	14.7±1.3 (1.4)
Norb9	NA1	46.896	13.350	1575	1	0.9560	22.27±0.79	15.7±0.6 (0.9)	15.9±0.6 (1.0)
Norb10	NB1	46.894	13.367	1931	1	0.9552	25.96±0.71	14.1±0.4 (0.8)	14.3±0.4 (0.8)
Norb11	NB1	46.893	13.366	1910	1.5	0.9621	23.19±0.67	12.8±0.4 (0.7)	12.9±0.4 (0.7)
Norb12*	NB2	46.894	13.362	1864	1.5	0.9736	24.85±1.24	14.0±0.7 (1.0)	14.2±0.7 (1.0)
Norb13	NC1	46.904	13.380	2335	1.5	0.9673	27.78±0.94	11.3±0.4 (0.7)	11.4±0.4 (0.7)
Norb14*	NC1	46.904	13.381	2342	1.5	0.9725	27.98±1.18	11.3±0.5 (0.7)	11.4±0.5 (0.7)

^a Shielding correction includes the topographic shielding due to surrounding landscape and the dip of the sampled surface.

^b AMS measurement errors are at the 1σ level. Sample ratios are normalized to the 07KNSTD standard.

^c Age errors are internal errors. External errors are given in parentheses.

^d Exposure ages have been corrected for a surface erosion rate of 1 mm ka^{-1}

* Blank correction value of $^{10}\text{Be}/^9\text{Be} = (6.62 \pm 1.37) \times 10^{-15}$, for the other samples a long-term laboratory blank of $^{10}\text{Be}/^9\text{Be} = (3.67 \pm 2.17) \times 10^{-15}$ was used.

d-c Glacier: debris-covered glacier.

(±0.8) ka for the Tandl site (Table 1, Fig. 3a) and 11.4 (±0.4) to 16.7 ± (0.9) ka for the Norbert site (Table 2, Fig. 3b). In line with previous authors (Barrows et al., 2004; Hippolyte et al., 2009; Ivy-Ochs et al., 2009; Moran et al., 2016; Andrés et al., 2018), we consider the exposure ages as final boulder stabilisation ages, which record the transformation from an active rockglacier into an immobile inactive or relict rockglacier. Samples from a single lobe gave consistent ages (Fig. 3). Ages of lobes decrease with increasing elevation. This suggests that the effects of inheritance, boulder rotation and rock fall are relatively minor at these sites. These topics

and the implications for exposure dating of rockglaciers are discussed in more detail below (see section 5.1). We combine the exposure age data with our detailed geomorphological analysis to decipher the morphological evolution of the Tandl and Norbert Valleys.

4.1. Tandl rockglaciers

The Tandl rockglaciers are situated along the northern slope of the steep mountain flank, between the Firstriegel (2007 m a.s.l.)

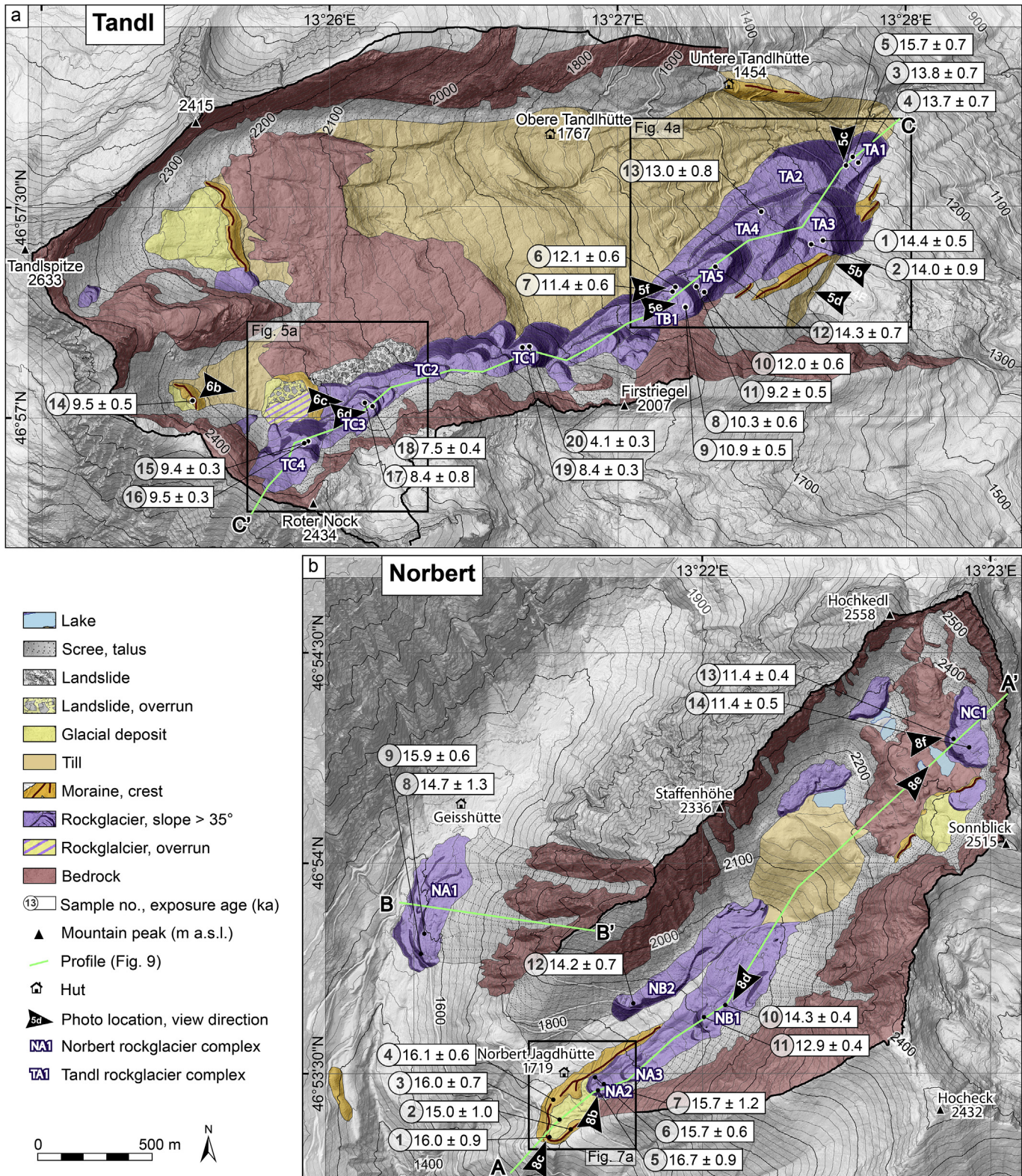


Fig. 3. Geomorphological maps of the Tandl and Norbert study sites. The maps show details of landforms and deposits of the Tandl and the Norbert study sites and determined exposure ages (erosion corrected). Background map is a slope map (using grey shades) overlain on a hillshade map, which are both based on a digital elevation model (1 m resolution). Black rectangles show the extent and the position of details shown in Figs. 4a, 5a and 7a. (For interpretation of the references to color in this figure legend, the reader is referred to the Web version of this article.)

and the Roter Nock (2434 m a.s.l.) (Fig. 3a). They are a ~3 km long, complex and continuous series of over 12 rockglacier lobes that appear to have partly overrun each other. The rockglacier surface is composed of very large (0.5–5 m) clast-supported boulders of Zentralgneiss. Only occasionally on the steep (>35°) front and side slopes fine sediments crop out. According to their morphology and exposure ages, the rockglaciers were grouped into the lower elevation complex TA, with lobes TA1–5 (Fig. 4a), the middle lobe TB1 and the higher elevation complex with lobes TC1–3.

The lowest lobe of the Tandl series (TA1) has a front slope of roughly 40 m in height and is located at an elevation of only 1220 m a.s.l. (Fig. 3a). Three samples (13.8 ± 0.7 ka (Tandl3, Figs. 4c), 13.7 ± 0.7 ka (Tandl4) 15.7 ± 0.7 ka (Tandl5)) of this lowest lobe suggest an active phase between 16–13 ka ago. The lobe is about

100 m wide, but only 200 m of its length is visible, as it was overrun by two other rockglaciers. On the left side, lobe TA1 is overrun by rockglacier lobe TA2, which is about 40 m thick, 200 m wide, over 1 km long and reaches up to an elevation of 1740 m a.s.l. TA2 was not dated. From the right side, rockglacier lobe TA3 overtops both TA1 and TA2. Exposure ages of 14.4 ± 0.5 ka (Tan1) and 14.0 ± 0.9 ka (Tan2) for lobe TA3 are in well agreement with each other and overlap with the two younger ages for lobe TA1. This suggests final stabilisation of the three lobes at about 14 ka.

The rockglacier front of TA3 is over 100 m high, and on its right side it is constrained by a 150 m long ridge, which was first thought to be part of the rockglacier. During fieldwork, it was realised that the ridge is too smooth to be a rockglacier feature, as there were no big boulders at all. At a road cut, a fresh outcrop was dug into the

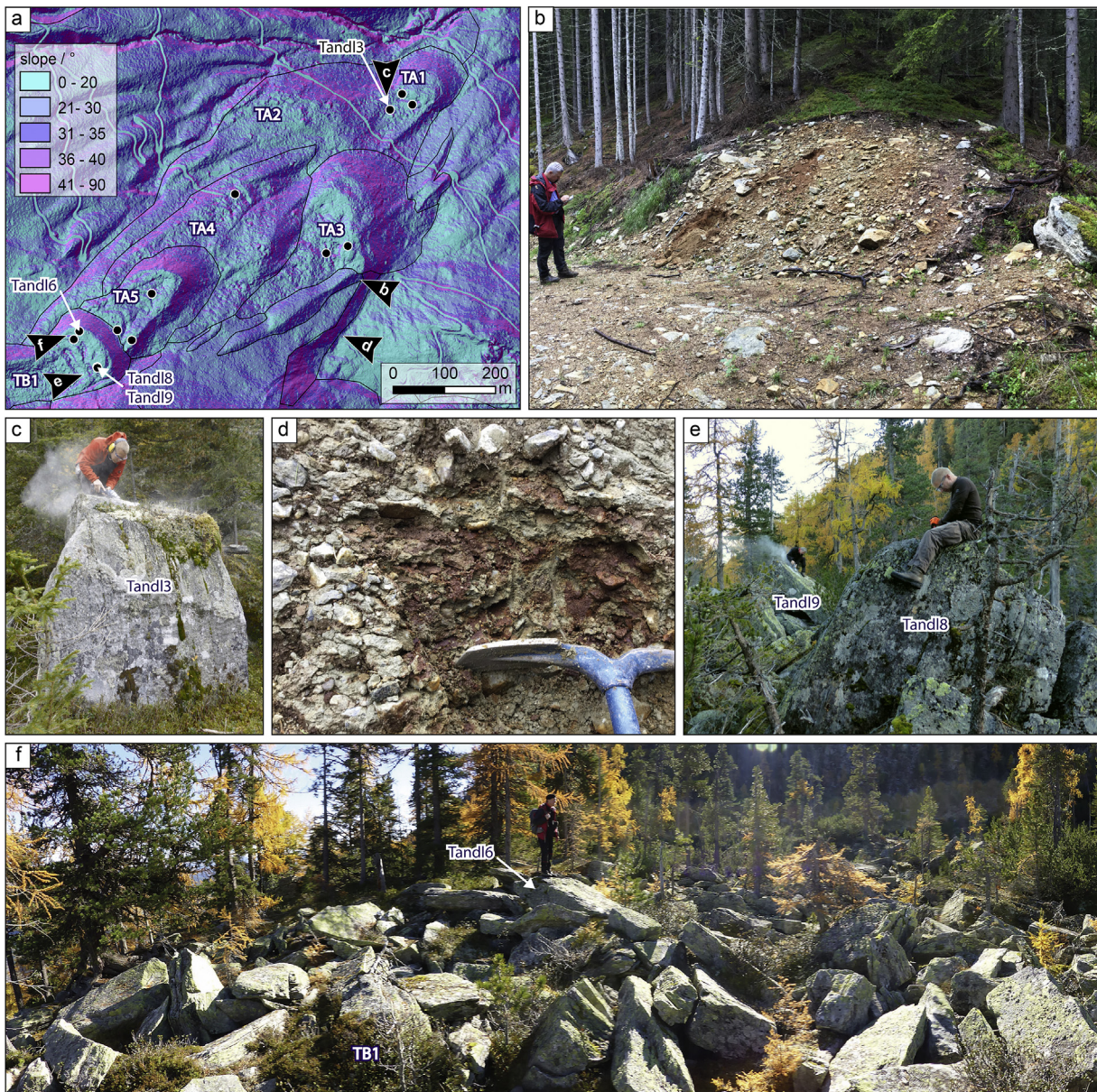


Fig. 4. Details and photographs of the lower part of the Tandl site. (a) Close-up of the TA rockglacier complex (for location see Fig. 3a). The slope map view highlights the steep rockglacier fronts and that the lowest rockglacier lobe (TA1) possibly is related to rockglacier lobe (TA4). Black dots show sample locations, only boulders shown on photographs are labelled, for names of the other samples see Fig. 3a. Black arrows indicate location and view direction of the photographs b–f. (b) Road cut through the moraine ridge. (c) Sampled boulder Tandl3. (d) Strongly consolidated subglacial till outcrop. (e) Sampled boulders Tandl8 and Tandl9. (f) Panorama view of the rockglacier lobe TB1 and sampled boulder Tandl6. (For interpretation of the references to color in this figure legend, the reader is referred to the Web version of this article.)

landform (Fig. 4a and b). The investigation revealed a matrix-supported, polymictic sediment with subangular to subrounded clasts that range from a few cm to 0.5 m in size in a matrix of silty sand. Following the ridge downhill, a sharp contact (within few meters) was observed, where it changes from the smooth ridge to a block field and further down, the smooth part reappears again. We interpret this to mean that this ridge is not part of the rockglacier, but is a moraine ridge formed by a glacier that filled the valley before the rockglacier lobes evolved and overtopped the moraine. A corresponding glacial deposit was observed on the opposite valley side, just below the Untere Tandlhütte (Fig. 3a). Around 50–100 m outside both moraine deposits (Fig. 4a) outcrops were found with a highly consolidated clay to silt size sediment with almost no clasts larger than a few centimetres (Fig. 4d). This is interpreted as subglacial till related to an even older glacier extent.

Rockglacier lobe TA4 has a front slope that is around 40 m high (Fig. 3a). The exposure age is slightly younger 13.0 ± 0.8 ka (Tandl13) than the exposure ages of TA3 and TA1, but still within the uncertainties. However, the combined hillshade-slope map (Fig. 4a), which is a slope map (using grey shades) overlain with a hillshade map, shows that the rockglacier snout is no longer continuous and it seems that part of the front has collapsed. From the position and direction of the collapsed structure of TA4, and the lowest dated lobe (TA1), it is likely that the two lobes are related, since width and location of the flow ridges match. Possibly the lower lobe (TA1), detached from the TA4 rockglacier lobe. Interestingly, the intermediate part, between TA1 and TA4 was covered by rockglacier lobes TA2 and TA3, indicating that the entire rockglacier complex TA1–4 (and also TA5, see below) was active at the same time, and according to the exposure ages also finally stabilised at the same time, around 14 ka ago. The only age that does not fit perfectly in this time is Tandl5 (15.7 ± 0.7 ka). The too old age might be a record of the early phase of rockglacier activity (cf. Moran et al. (2016)).

The exposure age of Tandl12 (14.3 ± 0.7 ka), on the overlying rockglacier lobe (TA5), suggests stabilisation around 14 ka which is roughly the same time when the lower elevation lobes (TA1–4) stabilised. The concentric shaped rockglacier lobe is around 100 m wide and 60 m high. To check the hypothesis that the stabilisation of a rockglacier lobe could also be dated by sampling boulders that fell down from the steep front during the last movement of the rockglacier (Haeberli et al., 2003), additionally two boulders were sampled on TA5 (Tandl10 and Tandl11), which lie just in front of the next higher rockglacier lobe TB1.

Indeed, the exposure ages of Tandl10 and Tandl11 (12.0 ± 0.6 ka and 9.2 ± 0.5 ka), agree well with the ages of the next higher rockglacier lobe TB1 (Tandl6 12.1 ± 0.6 ka (Fig. 4f), Tandl7 11.4 ± 0.6 ka, Tandl8 10.3 ± 0.6 ka (Fig. 4e), Tandl9 10.9 ± 0.5 ka). Therefore, sampling the very last fallen boulders could be another or complementary sampling strategy to date the stabilisation of relict rockglaciers. Overall, the six exposure ages (Tandl6–11) indicate stabilisation of lobe TB1 around 12–10 ka ago. The lobe defines a 600 m long, 100 m wide and 30 m high plateau that has well developed transverse ridges in the frontal part. The central part of the rockglacier body appears collapsed. The root zone of this lobe is in the talus slope below the Firstriegel (Fig. 3a), where also several small rockglacier deposits (undated) are found. Generally, it seems like all the rockglacier lobes described so far (complex TA,TB1) developed from the talus deposited at the foot of the Firstriegel.

The rockglacier lobes from here on upwards (complex TC) do not seem to have a single sediment source but were fed by the extensive talus slopes between the Firstriegel and Roter Nock (Fig. 3a). The steep front slope ($35\text{--}40^\circ$) of rockglacier lobe TC1 is 100 m high in comparison to the surrounding topography directly to the north and 80 m high where it slightly overtops rockglacier body TB1. Two

boulders were dated of TC1; Tandl19 8.4 ± 0.3 ka and Tandl20 4.1 ± 0.3 ka. Based on the ages from the previously mentioned lobes and the results from samples at higher elevation, which will be discussed below, we consider the Tandl20 age as an outlier (see also section 5.1).

The next higher rockglacier TC2, is actually a group of lobate-shaped rockglaciers. They were combined, because it seems like several lobes are stacked, which makes it difficult to distinguish between single lobes (Fig. 3a). This is also, why no samples were taken in this part. Just to the west and in part overlying the TC2 complex is rockglacier TC3. It is 260 m long, 120 m wide and has a well-formed 20 m high arcuate frontal wall (Figs. 3a and 5a,d). TC3 has a very well-developed furrow and ridge morphology but in comparison with the other rockglacier lobes described above, it is rather thin with a thickness of about 10 m (Fig. 5c). The debris source is the talus of the small cirque below Roter Nock (Fig. 3a). Two exposure ages suggest stabilisation of the tongue at around 8 ka (Tandl17 8.4 ± 0.8 ka (Fig. 5d), Tandl18 7.5 ± 0.4 ka), hence around the same time as rockglacier lobe TC1. The highest dated rockglacier of the Tandl Valley (TC4) is located in a cirque below Roter Nock. Its $35\text{--}40^\circ$ steep front slope rises about 70 m above the cirque floor (Fig. 5a). Two samples of the rockglacier body gave exposure ages of 9.4 ± 0.3 ka (Tandl15) and 9.5 ± 0.3 ka (Tandl16). These are discussed in further detail below in section 5.2.

In this upper part of the study site some other interesting landforms were observed (Fig. 5a). In front of the lobate shaped rockglaciers of complex TC2, a block field was observed with almost exclusively giant angular boulders (5–10 m). Since there were no clear front and side scarps with fine material and no signs of (past) creep, it was mapped as a landslide deposit. The landslide is partially covered by the rockglacier deposits of TC2, which is thus younger. Another enigmatic feature is the hummocky, grass-covered area in front of the rockglacier lobe TC4 (Fig. 5a and b). Only scattered boulders (<1 m) were found distributed on the maximally 1 m high gentle hills. From east to north, distinct parallel ridges rim the area (Fig. 5a, white line), which were interpreted as moraine ridges. Careful inspection of the aspect-slope map further allowed following the rockglacier-landslide contact below the glacially smoothed area, indicated by the arrows and the black (dashed) lines on Fig. 5a. We conclude, that a glacier advanced out of the cirque below the Roter Nock, covering the rockglacier and the landslide deposit (Fig. 5a, black dashed lines), smoothing the underlying landforms, by infilling glacial sediments into spaces between the boulders.

In the adjacent small cirque, a ridge shaped feature was observed (Fig. 3), composed of scattered blocks between 0.2 and 2 m in size in a sandy matrix. The mostly grass covered ridge is backfilled with talus. We mapped it as a moraine ridge due to the few big boulders, but it could also be a pronival rampart (cf. Scapozza (2015)), formed by rock fall deposits that were rolling or sliding across a perennial or late-lying snow patch (Hedding, 2011). A large boulder on the ridge gave an exposure age of 9.5 ± 0.5 ka (Tandl14). There are several small rockglaciers in the highest talus slopes (Fig. 3a) but they were not considered for dating, as recent rock fall events could not be excluded.

4.2. Tandl paleo-glacier reconstruction and ELA calculation

Reconstruction of the Tandl paleo-glacier (Fig. 6a) based on the mapped moraines and using GLaRe (Pellitero et al., 2016), suggests that the paleo-glacier was around 60–80 m thick and had a simple and flat appearance. This could be due to the rather gentle slope of the topography. Determined ELAs for the reconstructed paleo-glacier are 1920 m a.s.l. and 1880 m a.s.l., using an accumulation area ratio (AAR) of 0.60 and 0.65 respectively. To determine the

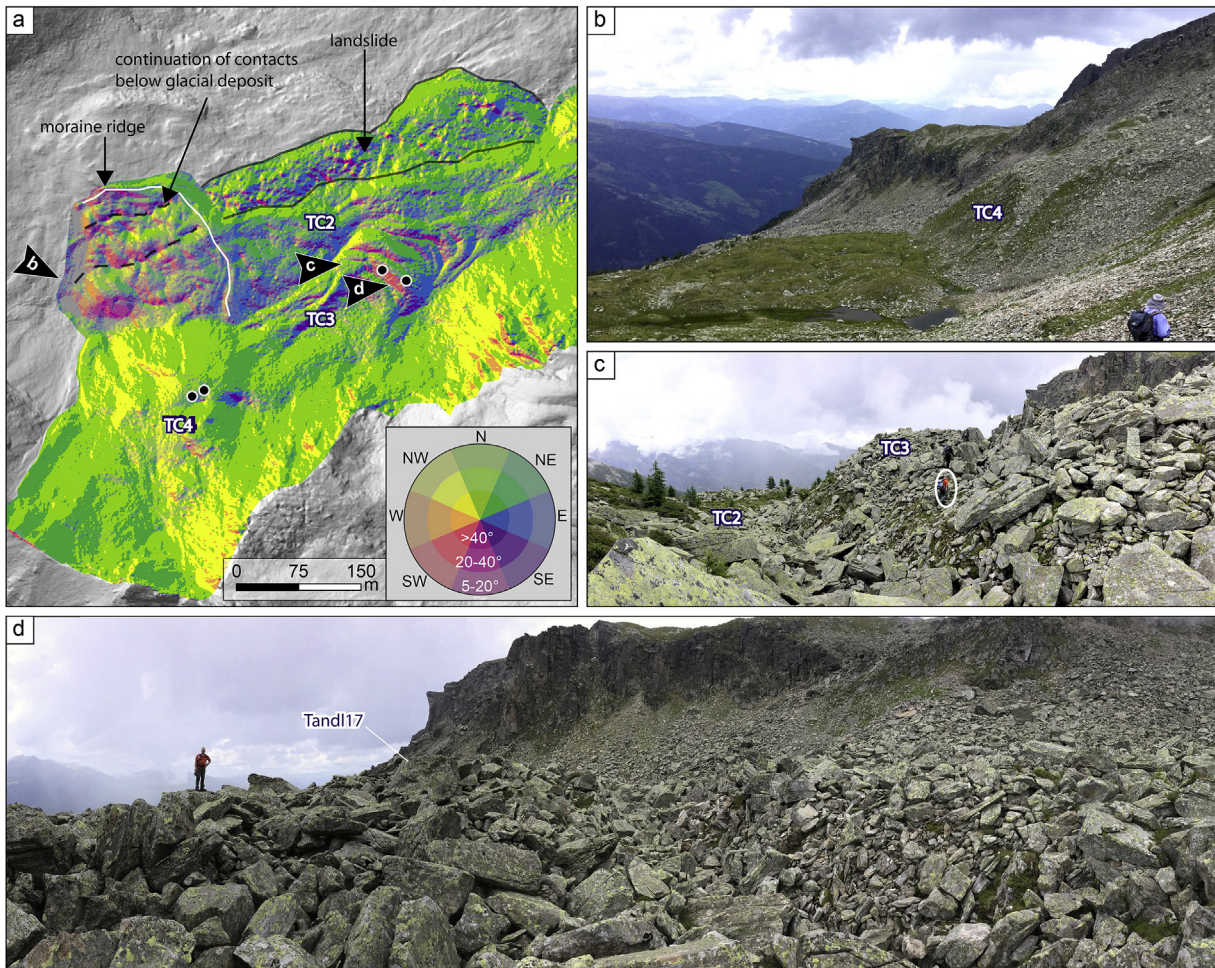


Fig. 5. Details and photographs of the higher part of the Tandl site (for location see Fig. 3a). (a) Slope-aspect map of the rockglacier complex TC2-4, highlighting the crosscutting relationship of the landforms. Black lines show the contact of the surrounding surface to the landslide deposit and from the landslide and the rockglacier deposit (TC2). The black dashed line emphasizes the continuation of the contacts below the glacially overrun part. Glacial extent is drawn as a white line. Black arrows indicate location and view direction of the photographs b-d. (b) View down to the glacially smoothed and vegetation covered area, and the 70 m high rockglacier front slope of TC4. (c) View from an older rockglacier deposit (TC2), with single trees growing between the boulders, towards the side slope from a younger rockglacier lobe with absolutely no vegetation on top (TC3). Person encircled for scale. (d) Panorama taken on top of rockglacier TC3 showing the sampled boulder Tandl17 and the typical, very blocky appearance of the Tandl rockglaciers. (For interpretation of the references to color in this figure legend, the reader is referred to the Web version of this article.)

Δ ELA for the Tandl paleo-glacier, which is the difference between the local ELA during the Little Ice Age (LIA) and the paleo-ELA, the LIA-ELA of the Ankogel (Fig. 1b) with an average of c. 2700 m a.s.l. (Lieb, 1993) was used, as the Tandl Valley was not glaciated during the LIA (Gross and Patzelt, 2015). The calculated Δ ELA is approximately -800 m. Kerschner et al. (1999) suggested a lowering of the ELA position of about -700 m during the Gschnitz stadial, in the Gschnitz Valley (Fig. 1b). Similar values between -650 m and -700 m were determined for Gschnitz stadial glaciers in several other locations in the Eastern Alps (Ivy-Ochs et al. (2006a), and references therein). Based on this we interpret the moraines in the Tandl Valley as having been deposited by the local Gschnitz stadial glacier (there were no boulders suitable for exposure dating).

4.3. Geomorphologic and paleoclimatic history of the Tandl Valley

Our combining of geomorphological observations and exposure ages shows that during the Lateglacial and early Holocene there were several quasi-contemporaneous phases of glacier and

rockglacier activity in the Tandl Valley. The main findings are summarised in Fig. 6.

The oldest sediment is the strongly consolidated subglacial till that outcrops distal to the Gschnitz moraine ridges (Fig. 4d). Although the age of deposition is difficult to constrain, the position external to the Gschnitz moraines requires a pre-Gschnitz age, thus the till is attributable to the early Lateglacial or even to the LGM. The reconstructed paleo-glacier defined by the mapped moraines (Fig. 6a) and the calculated Δ ELA show that the valley was covered by a local Gschnitz glacier. With the disappearance of the glacier, permafrost developed and formation of the TA-rockglacier complex started (Fig. 6b). According to our ^{10}Be exposure ages of the TA rockglaciers, the first phase of rockglacier activity ended around 14 ka (Tandl1-5, Tandl12-13). This suggests that the Gschnitz stadial glacier wasted rather rapidly, probably within only a few decades. Firstriegel must have been a very active mountain slope with numerous rock falls, producing abundant talus to constantly feed the over 1 km long TA rockglacier complex. Today the E-W trending rock wall with the Firstriegel is still known for frequent rock fall activity (Schuster et al., 2006). The lowest elevation of the TA

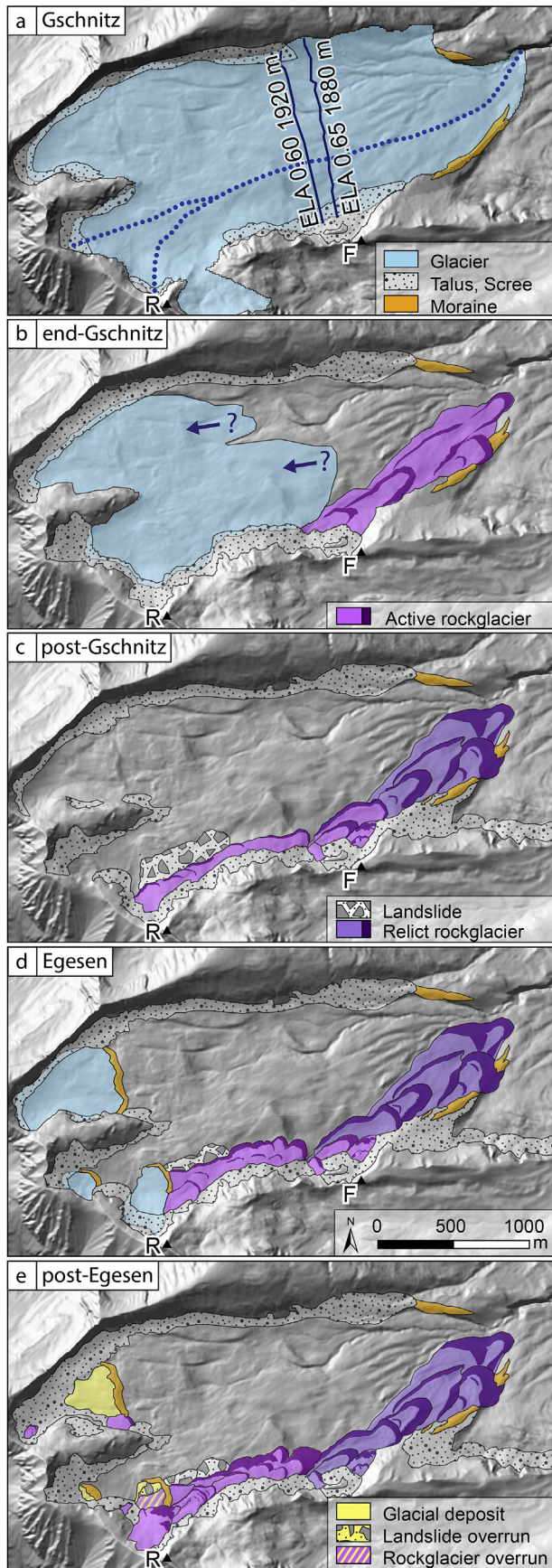


Fig. 6. Reconstructed geomorphological history of the Tandl site. (a–e) Summarises the evolution of the glacier and rockglaciers in the area from the local Gschnitz stadial

complex, around 1350 m a.s.l., represents the lower limit of permafrost, or the $-2\text{ }^{\circ}\text{C}$ isotherm, in this post-Gschnitz time around 14 ka ago. Modern day MAAT at this elevation is approximately $4.3\text{ }^{\circ}\text{C}$, hence the temperature difference from today compared to post-Gschnitz paleoclimate at around the transition to the Bølling Interstadial is around $-6.3\text{ }^{\circ}\text{C}$.

With ongoing glacier recession the highest parts of the Tandl Valley became ice-free, and probably soon after disappearance of the ice the landslide occurred (Fig. 6c). Within a short time, rockglacier formation was initiated, as rockglacier deposits moved onto the landslide deposit. It is likely that rockglaciers developed not only at high elevation but also all along the mountain flanks down to the Firstriegel (lobes TC4-TB1, Figs. 4,6c). Based on the exposure ages between 12–10 ka the activity of the lowest of these rockglaciers (TB1) ended around the end of the Younger Dryas cold phase (Fig. 6d). Furthermore, samples dates Tandl6–11 suggests that during the Younger Dryas the lower limit of discontinuous permafrost, and the $-2\text{ }^{\circ}\text{C}$ isotherm were located around 1700 m a.s.l. Calculating the temperature depression with a modern MAAT of $2.6\text{ }^{\circ}\text{C}$ at that elevation results in a temperature lowering of approximately $-4.6\text{ }^{\circ}\text{C}$ for the Egesen stadial.

The observed moraine deposits below the Roter Nock are assigned to the Egesen stadial (Fig. 6d), based on geomorphological field evidence, the exposure age of Tandl14, and their comparable elevation to Egesen extents mapped at the Seebach Valley (Fig. 1b) (Grischott et al., 2017; Drescher-Schneider and Reitner, 2018). During its advance the Tandl Egesen stadial glacier below the Roter Nock overran both rockglacier and landslide deposits (Fig. 6d). Exposure ages and these cross-cutting relationships suggest that during the Younger Dryas, small Egesen glaciers and rockglaciers co-existed in the Tandl Valley above elevations of about 2200 m a.s.l. It is likely that towards the end of the Younger Dryas, Roter Nock provided enormous amounts of debris, which led to initiation of rockglacier TC4.

The exposure ages of Tandl17–19 (TC1, TC3), which are all around 8 ka are surprisingly young. The ages fall within the Holocene Climate Optimum, when temperatures are thought to have been warmer than present (Heiri et al., 2014; Solomina et al., 2015). Our interpretation is that these exposure ages record extremely slow degradation of the rockglaciers, due to slow melting of the interstitial ice (Fig. 6e) (see also below). Exposure ages suggest that lobe TC4 stabilised before the rockglacier lobe that it partially covers (TC3). TC4 may have become topographically inactive when it reached the flat part of the cirque (Fig. 5b). On the other hand, all of the TC lobe ages may have been affected by instabilities related to (partial) reactivation during late Holocene cold periods. In light of the young ages, we considered it conceivable that parts of the highest rockglaciers (~ 2300 m a.s.l.) could still contain ice, even though the present day permafrost limit is at 2600 m a.s.l. To check for any movements we used image correlation analysis (Messierli

glacier to the situation after the Egesen stadial. F: Firstriegel, R: Roter Nock. (a) The extent of the reconstructed local Gschnitz glacier (see section 3.2). Dotted line shows the flowline used for the paleoglacier reconstruction. The two blue lines across the glacier are the calculated ELA positions using the AAR method with a ratio of 0.60 and 0.65. (b) Immediate advance of the rockglacier into the deglaciated area. Question marks indicate that the exact location of the glacier front is unknown. (c) During the ongoing warming, the lowest rockglacier became inactive (relict) and it is likely that the Gschnitz glacier disappeared completely as indicated by the landslide deposit and the evolution of the lobate shaped rockglaciers all along the mountain flank. (d) Climate deterioration of the Younger Dryas led to formation of cirque glaciers. The rockglaciers in the higher parts remained active. (e) Egesen stadial glaciers disappeared due to the warming of the early Holocene while rockglaciers above 1900 m a.s.l. remained active (boulders not fully stabilised) until the early Holocene. (For interpretation of the references to color in this figure legend, the reader is referred to the Web version of this article.)

and Grinsted, 2015). Orthophotos from the years 2003 and 2013 were compared using the ImGRAFT feature tracking tool. The results show that there was no significant horizontal movement or collapse (ice melt) of the highest rockglaciers over the 10 years between the photos.

4.4. Norbert rockglaciers

The Norbert rockglaciers are not a continuous series of rockglaciers like the Tandler rockglaciers, but comprise several separate landforms at different elevations (Fig. 3b). The rockglacier deposits are exclusively composed of large Zentralgneiss boulders ranging up to 5 m in size (Fig. 7d) and are often even lacking a matrix of fines in the frontal slopes (Fig. 7b,f). The rockglacier lobes were arranged into three groups based on their position and the determined exposure ages; the lowest and oldest rockglaciers NA1-3, the next higher group NB1-2, and the highest and youngest rockglacier NC1.

About 1 km south and downvalley of the Geisshütte (Fig. 3b), several parallel, vegetated soft ridges were observed. Inspection of an outcrop showed that the ridge is composed of unsorted, fine-grained sediment with few clasts larger than 50 cm. Based on sedimentology, location, orientation and shape of the landform we interpret the ridges to be remnants of a lateral moraine. Close to the Geisshütte at an elevation between 1580 and 1600 m a.s.l., a lobate shaped, about 550 × 180 m large and very blocky deposit was mapped as the lowest Norbert rockglacier body NA1. The hillshade and slope maps revealed that there are probably two to three rockglacier lobes stacked, with front slope heights of around 5–15 m and a total thickness of about 30–40 m. The debris sources are two channels and their talus fans located southwest of the Staffenhöhe (Fig. 3b). Our obtained exposure ages suggest stabilisation of these rockglaciers between 15.9 ± 0.6 ka (Norb9) and 14.7 ± 1.3 ka (Norb8). The former age may plausibly be considered an age for onset of rockglacier movement (section 5.1).

The next investigated landforms are situated in the somewhat higher side valley to the east, close to the Norbert Jagdhütte (Figs. 3b and 7a). The hillshade map shows a complex landform consisting of at least five tongues, extending from ~1700 m–2000 m a.s.l. Previously they were all mapped as rockglacier lobes (Reitner, 2007b). However, field observations offered several arguments that the lower two lobes are remnants of a debris-covered glacier. Sediment analysis of outcrops showed, that the material is a diamicton with a silt-rich matrix with some clay, and angular but also many subrounded clasts, all <50 cm in size. Furthermore, the surface morphology is less blocky than NA2 and only scattered boulders are found; those larger than 1 m are rare (Fig. 7c). The central part of the deposit displays a chaotic mixture of collapsed structures, hummocky features and minor incised stream channels (Fig. 7a), but no distinct flow-like features were observed. Based on this evidence the lower part of the complex was interpreted as a debris-covered glacier deposit and we mapped the enclosing rim as moraines. Exposure ages of four boulders, three on the moraine ridge (Norb1 16.0 ± 0.9 ka (Fig. 7c), Norb2 15.0 ± 1.0 ka and Norb4 16.1 ± 0.6 ka) and one from the central part (Norb3 16.0 ± 0.7 ka) suggest a maximal extent of the glacier around 16 ka. Interestingly, the debris-covered glacier was not flowing along the valley bottom but was located on the eastern side of the valley. A plausible explanation is the annual sunshine duration. Due to the high and steep headwall there is less sunshine on the northwest-facing than on the southeast-facing valley side (Fig. 2). Furthermore, the steep slope to the southeast (up to 400 m high) presumably provided abundant debris onto the glacier's ablation area, which acted as insulation and reduced ice-melt (Mattson et al., 1993; Pratap et al., 2014).

About 300 m upslope from the terminal moraine (Fig. 7a) of this debris-covered glacier deposit, there is a very distinct change of surface morphology, from relatively smooth to extremely blocky. Rockglaciers NA2 and NA3 lie right on top of the debris-covered glacier deposit. Lobe NA2 is 10–15 m high with a >35° steep front, and is composed of large (>0.5 m) angular, interlocked blocks (Fig. 7b). In addition, meter sized unstable boulders dominate the flat part on top. On the hillshade-slope map indications of transverse ridges can be seen (Fig. 7a), suggesting that this is the snout of a rockglacier lobe (NA2). Exposure ages of 16.7 ± 0.9 ka (Norb5), 15.7 ± 0.6 ka (Norb6) and 15.7 ± 1.2 ka (Norb7) suggest stabilisation of this rockglacier lobe (NA2) around 15.7 ka. The 16.7 ka age may record onset of rockglacier movement (section 5.1).

Lobe NA3 is located 100 m upvalley from NA2 (Fig. 7a). No boulders suitable for dating were found. Along the right-hand margin of rockglacier lobes NA2 and NA3, the right lateral moraine of the debris-covered glacier deposit is evident (Fig. 7a). It exhibits a much smoother morphology than the relict rockglaciers, has fewer and much smaller boulders, and occasionally a fine-grained matrix can be observed between the vegetation. It seems as if the moraine was constraining the rockglacier lobes in the lower part. Above 1860 m a.s.l., the moraine ridge disappears below the rockglacier deposits (Fig. 7a). On the hillshade and slope map, faint indications suggest continuation of the moraine ridge, for another ~100 m (horizontal distance) below the rockglacier.

Another 60 m upvalley (Fig. 3b), on top of the 25 m high rockglacier lobe (NB1), two boulders (Norb10 (Fig. 7d), Norb11) give exposure ages of 14.3 ± 0.4 ka and 12.9 ± 0.4 ka, respectively. Approximately on the same elevation (1830 m a.s.l.) but on the opposite valley side, there is another rockglacier deposit (NB2, Fig. 3b), which is 700 m wide. The downvalley front is almost 50 m high. The exposure age (Norb12) of a giant boulder (>6 m) on this rockglacier lobe (NB2) suggests stabilisation at 14.2 ± 0.7 ka. Rockglacier lobes NB1 and NB2 hence stabilised between 14 and 13 ka ago.

Both NB1 and NB2 start from a trough-floor area between 2010 and 1950 m a.s.l.; then they diverge, with NB1 under the WNW-facing slope, and NB2 under the SE-facing slope (Fig. 3b). Followed by a distinct 100–150 m high bedrock step above 2000 m a.s.l., which is covered by a layer of inferred glacial deposits, which are not well exposed. The area on top of the bedrock step (2140 m a.s.l.) is further divided by a 50–100 m high, valley-parallel bedrock cliff into a western and eastern part. West of the cliff, there are two cirque-shaped areas one lower and one higher. Both host lobate-shaped rockglaciers and lakes in their fronts. Despite their cirque-like shape, no distinct glacial landforms, like moraine ridges, were observed. The eastern part of the cliff is not cirque shaped but is rather a bedrock high (plateau-like area), with a very thin grass cover, and frequent outcropping of bedrock. Below the Sonnblick there is a complex landform (Fig. 3b). It is probably a combination of (debris-covered) glacier and periglacial deposits. Single identified landforms are a moraine ridge in two parts which can be followed all along the mountainside until the end of the area, and a rockglacier at the highest part. The ridge increases in height from 5 m at 2320 m a.s.l. to 10 m at 2290 m a.s.l. The moraine is composed of a considerable amount of fines, and only few boulders are larger than 1 m. Field observations show that in the upper part, the moraine confined the rockglacier lobe, which overtops the moraine lower down. Due to unclear boundaries and relations of the landforms, it was decided to not sample this complex landform.

The highest part of the valley, at around 2300 m a.s.l., hosts a 20–40 m thick, 170 m long and 330 m wide lobate shaped rockglacier deposit (NC1) (Figs. 3b and 7e,f). There is only patchy grass growing on the steep front slope, and boulder sizes range between 0.5 m and 5 m. Like the two rockglacier lobes in the small cirques in

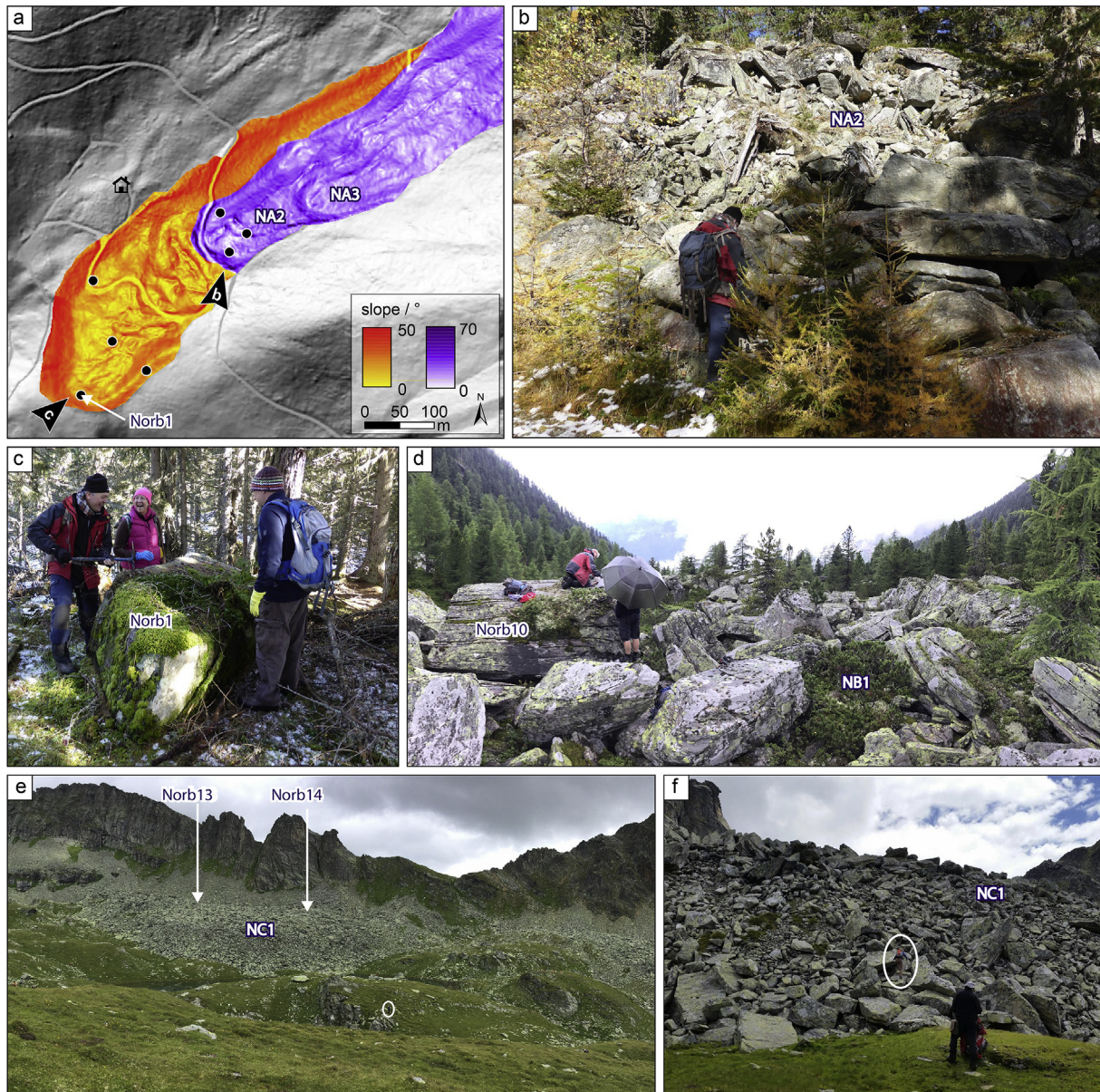


Fig. 7. Details and photographs of the Norbert site (for location details see Fig. 3b). (a) Slope map of the debris-covered glacier deposit (yellow-orange) and the rockglacier lobes NA2 and NA3 (violet), highlighting the difference of the hummocky and irregularly collapsed morphology of the debris-covered glacier deposit and the collapsed well-defined rockglacier lobes on top. Black arrows indicate location and view direction of the photographs b-f. (b) Photograph taken towards the front slope of the rockglacier lobe NA2. (c) Sampled boulder (Norb1) of the frontal moraine of the debris-covered glacier. Note that the surrounding of the boulder is not blocky. (d) View downvalley of rockglacier lobe NB1 and sampled boulder Norb10. (e) Panorama of the higher part of the Norbert site, with the rockglacier lobe NC1. Person for scale in the white circle. (f) Close-up of the front slope of the ~30 m high rockglacier NC1, person encircled for scale. (For interpretation of the references to color in this figure legend, the reader is referred to the Web version of this article.)

the western part, this rockglacier has a small lake in front of it. The two analysed samples have almost exactly the same exposure ages 11.4 ± 0.4 ka (Norb13) and 11.4 ± 0.5 ka (Norb14).

4.5. Geomorphologic and paleoclimatic history of the Norbert Valley

The dated deposits of the former debris-covered glacier (~16 ka), close to the Norbert Jagdhütte, indicate that the deposits are remnants of the local Gschnitz stadial glacier. Therefore, it is likely that a Gschnitz glacier also formed the lateral moraine remnant in the adjacent valley, approximately 1 km down-valley of the Geisshütte (Fig. 8a). As shown by the rockglacier deposit NA1 and its stabilisation ages around 15–16 ka, the local Gschnitz glacier must have

already retreated shortly after 16 ka to an elevation above the position of the rockglacier lobe ~1800 m a.s.l. (i.e. near the Geisshütte) (Fig. 8b). As in Tendl Valley, it is probable that significant debris had already accumulated on the surrounding slopes, perhaps blocked by the Gschnitz glacier. The same is implied by the rockglacier deposit NA2, located on top of the debris-covered glacier deposit (Fig. 8a), and the exposure ages of both landforms. The rockglacier NA2 is, with stabilisation ages of ~15.7 ka (NA2), only slightly younger compared to the exposure ages of the debris-covered glacier deposit (~16 ka). It is therefore likely that also here abundant debris from the large talus slope was already accumulating along the sides of the Gschnitz stadial glacier (Fig. 8a). Some of the debris must have covered the glacier and thus led to the debris-covered glacier, but probably much of the debris was impeded by the glacier, possibly

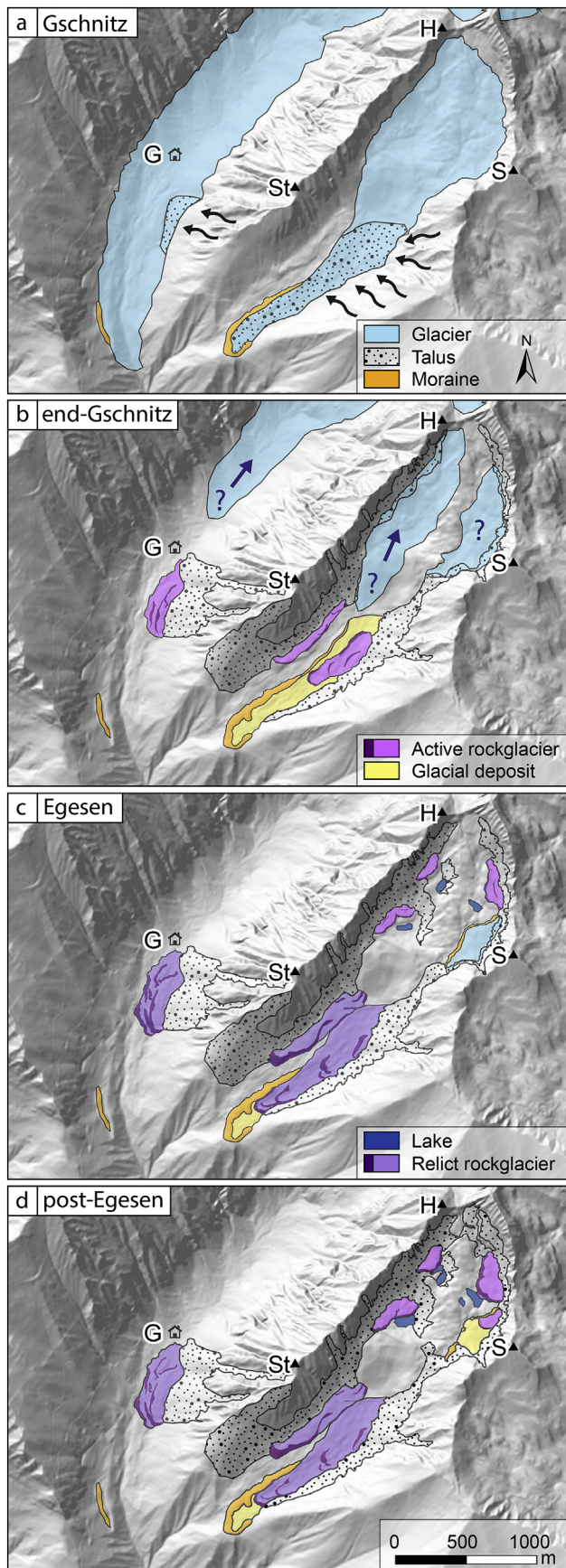


Fig. 8. Reconstructed geomorphological history of the Norbert site. (a–d) Summarises the evolution of the glacier and rockglaciers in the area from the local Gschnitz stadial

already under permafrost conditions. The short time difference between the landforms strongly suggests that rockglacier formation might have started simultaneously with the ice-decay of the debris-covered glacier, or shortly thereafter (Fig. 8b). However, final stabilisation of the rockglacier likely occurred after the debris-covered glacier had lost its underlying ice. If the several-meter-thick massive ice body of the debris-covered glacier would have melted after rockglacier stabilisation on top, the rockglacier surface would probably appear more collapsed, with something like kettle holes. However, the rockglacier seems neither extremely collapsed nor were kettle holes observed (Fig. 7a). Hence, we conclude that the rockglacier was still active while the debris-covered glacier ice melted, or it overran it after the ice had melted (Fig. 8b). The stabilisation position of the rockglacier deposits NA1 and NA2 suggest, analogously to the Tandl site, a temperature depression of $5.2\text{ }^{\circ}\text{C}$ for NA1, using a modern MAAT at 1580 m a.s.l. of $3.2\text{ }^{\circ}\text{C}$, and for NA2 a lowering of $-4.5\text{ }^{\circ}\text{C}$, applying a modern MAAT of $2.5\text{ }^{\circ}\text{C}$ at 1730 m a.s.l. The stabilisation ages of the rockglacier lobes on both valley sides NB1 and NB2 around 1900 m a.s.l., suggest an extended activity into the Bølling-Allerød and an increase in the elevation of the permafrost limit around 14–13 ka ago.

The last indicator of permafrost occurrence in the Norbert Valley is given by the highest (~ 2300 m a.s.l.) rockglacier NC1. This rockglacier stabilised at 11.4 ka likely with the termination of the Egesen stadial (Fig. 8c). Because the rockglacier advanced into a flat area, it is not entirely clear whether it became climatically or topographically inactive. Hence, we refrain from making a conclusive statement about the elevation of the permafrost limit during the Egesen. Landforms possibly related to an Egesen glacier were only found in the northwest facing part below the Sonnblick, which is well shaded (Fig. 2).

5. Discussion

5.1. Implications for cosmogenic nuclide dating of rockglacier deposits

There is considerable discussion on how to interpret exposure ages of relict rockglaciers (Haerberli et al., 2003; Winkler and Lambiel, 2018; Knight et al., 2019). One major concern is inheritance (pre-exposure), which would lead to too old exposure ages. But where could such inheritance come from and how much could it be? It can be assumed that LGM glaciers effectively cleared away all the debris from the high mountain areas and eroded more than several meters from the bedrock (Wirsig et al., 2016, 2017). This makes it rather unlikely to have inheritance that was acquired before or during the LGM. The question remaining is how fast and how far back glaciers had retreated before they re-advanced during the Gschnitz stadial. In any case, maximal inheritance acquired post-LGM but pre-Gschnitz would correspond to only 1000–2000 a. Additionally, rockglacier dynamics (Barsch, 1992; Haerberli et al., 1998; Hoelzle et al., 1998; Arenson et al., 2002; Springman et al., 2012) make it almost impossible to integrate or to move blocks, which were left by (debris-covered) Gschnitz stadial glaciers, from the valley floor up to the position on top of the rockglacier where

glacier to the situation after the Egesen stadial. H: Hochkedl, S: Sonnblick, St: Staffenhöhe, G: Geissshütte. (a) Gschnitz glaciers are covering the valleys. Abundant talus from the hill-slopes (black arrows) covers lower parts of glaciers. (b) Retreat of the Gschnitz glacier, but their precise position is unknown as indicated by the question marks. From debris accumulations the first rockglaciers develop. (c) During the Younger Dryas the lower rockglaciers became inactive, but at higher elevations, many new rockglaciers developed. Only in the well-shaded part did a small Egesen stadial glacier form. (d) Egesen rockglaciers above 2150 m a.s.l. appear to have remained active into the mid-Holocene. (For interpretation of the references to color in this figure legend, the reader is referred to the Web version of this article.)

we sampled boulders. The caterpillar-like movement of a rockglacier, creeps gently over structures rather than destroying or incorporating them (Haeberli, 1985). Finally, talus-derived rockglaciers develop below very active mountain flanks, which produce abundant blocky material, thus pre-exposure from the headwall also seems unlikely (Barrows et al., 2004; Ivy-Ochs et al., 2009). On the other hand, there are two boulders (Norb5 on lobe NA2 and Tandl5 on lobe TA1) that have ages which are slightly older (<1000 a) than the other boulders on the same rockglacier lobe (Fig. 3a and b). This small offset could be an indication of the early phase of rockglacier formation (cf. Barrows et al. (2004); Moran et al. (2016)). It is thought that boulders that fall on the apron of the rockglacier are slowly transported on the rockglacier surface to its front, while during transportation the boulders are unstable, likely frequently turning or rotating. This instability of the boulder during movement could explain a certain (but small) scatter in exposure ages, where some sampled surfaces were longer exposed during transport and others less.

Clearly too young exposure ages can indicate fresh rock fall onto the rockglacier or instability and rotation of the boulder at a later stage, which could almost happen to every boulder as in general a rockglacier is a very unstable construct. However, of our 34 samples only one boulder had a clearly too young exposure age (Tandl20: 4.1 ± 0.3 ka). Young outliers due to fresh rock fall can be avoided by careful selection of boulders that have a reasonable distance from the source in the active steep wall (cf. Andrés et al. (2018)).

5.2. Insights into rockglacier morphodynamics and rockglacier-glacier interaction

Our detailed study of the complex structure of the Tandl and Norbert rockglaciers, together with the new 34 new boulder stabilisation ages, allows us to gain insight into rockglacier morphodynamics and evolution. Information gleaned relates to the size, shape, velocity as well as inter-lobe interactions. Both lobate and tongue-shaped rockglaciers are common in the two study valleys. The distinction lobate vs. tongue-shaped is based on whether the landform is morphologically continuous with the foot of the talus slope or if it is detached from it and has moved downhill, respectively (Barsch, 1996; Ballantyne, 2018).

Several tongue-shaped rockglaciers characterize the TA complex in Tandl Valley (Fig. 3a). This complex had approximately 2 ka to develop and move down slope. This is based on the interpreted time of decay of the local Gschnitz glacier (about 16 ka), as well as the oldest age on the lowest lobe (Tandl5, 15.7 ± 0.7 ka on TA1), which may mark rockglacier onset, and the final stabilisation at around 14 ka shown by the other six dates. Within this time, the TA rock glaciers formed a 1 km long, multi-lobe and tongue-shaped rockglacier complex that was no longer connected to the talus slope. Based on the 2 ka-long active phase and an approximate length of ~1 km (Fig. 3a), an average creep rate of 0.5 m/a is obtained. This is well comparable to values measured at active rockglaciers in the Alps (Kääb et al., 2003; Kellerer-Pirklbauer and Kaufmann, 2018).

At higher elevation in the Tandl Valley the Egesen rockglaciers (TB1 and TC1–4), especially the ones below the ELA of the local Egesen stadial glacier (<2200 m a.s.l.), had at least the entire Younger Dryas cold phase (12.9–11.7 ka) to evolve (Fig. 3a). These rock glaciers are lobate shaped (except TB1 and TC3) probably due to the gentle slope <20°. Below 1800 m a.s.l. where the valley is steeper (20–30°) the rockglaciers are tongue shaped (TA, TB1). It also might be that if rockglaciers creep into a flat area, it does not move much further but eventually gets thicker instead (e.g. TC4, NC1). Therefore, the simple conclusion that longer tongues were active longer may not apply.

In the Tandl and Norbert Valleys, there are several examples of overriding lobes. Complex TA is composed of at least four rockglacier lobes, which all formed and stabilised within the same cold phase. In light of the exposure ages, it appears that an overriding rockglacier lobe does not necessarily indicate a new younger climate cold pulse or fluctuation of the permafrost limit (Frauenfelder and Kääb, 2000). The drivers behind formation of several lobes some of which override each other relate to topography, elevation and gradient as well as factors specific to each rock glacier such as its ability to overcome shear stress (Barsch, 1996). Finally, pulses in sediment delivery may cause a lobe that is closer to the talus slope to become more active and override lobes that are farther away from the talus slope (Merz et al., 2015). An enigmatic case of overriding is rockglacier lobe TC4 (~9.5 ka) which overrides TC3 (~8 ka). TC4 seems to have stabilised before the rockglacier lobe that it is partially covering (TC3). Based on the exposure ages we conclude that TC4 became topographically inactive when it reached the flat part of the cirque, where TC3 on the other hand was still able to move further down slope.

In the Norbert Valley, rockglacier lobe NB1 overran the deposit left after downwasting of the debris-covered glacier (Gschnitz stadial) (Figs. 3b and 7a). Nevertheless, morphological and sedimentological evidence speak against development of rockglacier NB1 out of the material of the debris-cover glacier deposit. On the contrary, the rockglacier lobe NB1 and the small rockglacier lobe, which seems to have just started developing below the talus slope (located near the arrow 8d in Fig. 3b), suggest that the rockglacier lobes are completely talus derived.

In the Tandl area (Fig. 3a), the rockglacier lobe TA3 is first constrained by the lateral moraine, then as soon it reached the level of the moraine it overtopped and buried part of it. No signs of the rockglacier damaging, destroying or incorporating the moraine were observed.

5.3. Lateglacial to early Holocene climate in the Eastern Alps

Based on our established rockglacier sequence chronologies for the two valleys we can now compare the two sites for spatial similarities and differences. The profiles across the rockglacier deposits from the Norbert rockglaciers to the Tandl rockglaciers (Figs. 3 and 9) allow an examination of the two sites with respect to their aspect, elevation and timing of stabilisation. As intuited, rockglaciers developed predominantly on the valley sides where annual sunshine duration is lowest (Fig. 2). In the Tandl area this is on the north facing slope below the mountain flank and in the Norbert area mainly on the northwest facing slopes. Although the morphological development of the two valleys is quite similar, the profiles drawn along the rockglaciers (Fig. 9) point to a striking elevation offset between the Tandl and the Norbert sites. Rockglaciers on the Tandl site that stabilised simultaneously with rockglaciers at the Norbert site, are located about 300–400 m lower. This clear difference probably shows the effect of the aspect. Our data shows that the Tandl rockglaciers with a northerly aspect stabilised after the Gschnitz stadial thus somewhat later and at lower elevations (1350 m a.s.l.) in comparison to the lowest elevation Norbert rockglaciers (1560 m a.s.l.) with a southerly aspect. An offset of 350–400 m related to aspect is reported for active rockglaciers in the Alps (Noetzli et al., 2007).

Our reconstructions of morphological development of the two study valleys can now be viewed in light of regional and Alps-wide climate variations during the Lateglacial and early Holocene. Key records for understanding Lateglacial paleoclimatic development in the Eastern Alps are Lake Jeserzensee and Lake Längsee (Schmidt et al., 1998, 2012; Huber et al., 2010), both sites are located just a few tens of kilometres from our study sites (Fig. 1b). The lake

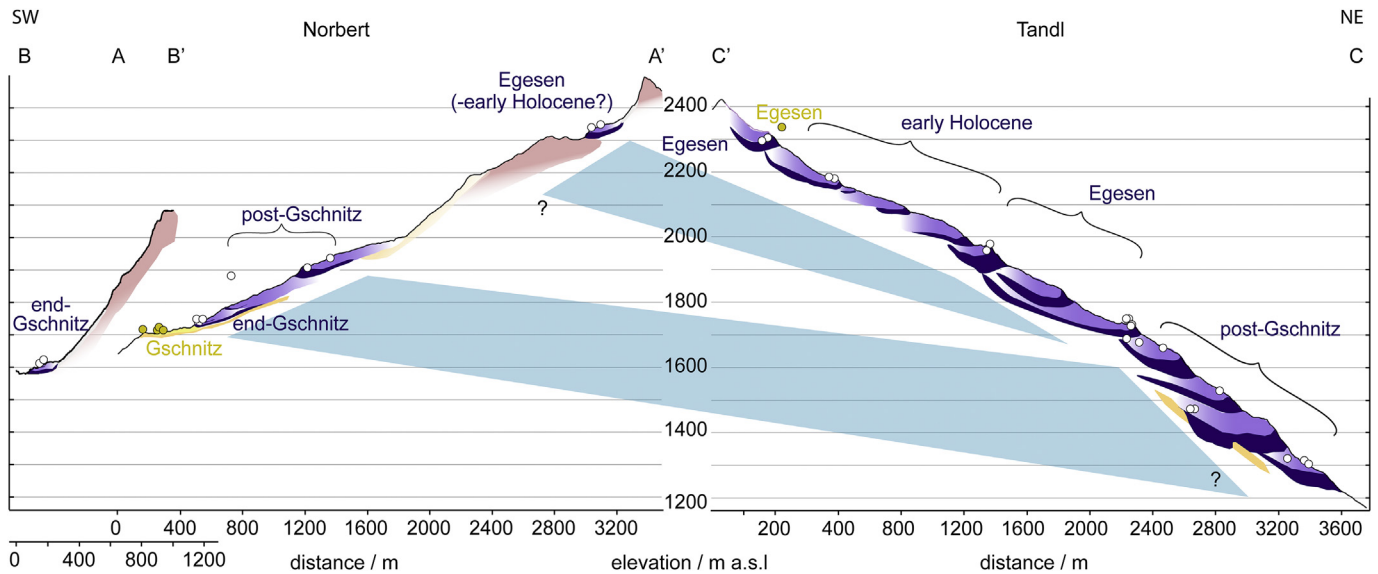


Fig. 9. Profiles across the rockglaciers. Profiles from southwest, across the Norbert rockglacier (A-A', B-B') with a southwestern aspect, to the northeast, across the Tandl rockglaciers (C'-C) with a northeastern aspect. Exact location of the profiles and color-codes of the landforms are shown in Fig. 3. This schematic side view of the rockglacier lobes, highlights their lateral boundaries. Blue shaded wedges show the approximate lower permafrost position during the stabilisation phases of the rockglacier deposits. Note the clear elevation offset between the two sites, with the rockglacier with north exposure being several hundred meters lower in elevation during each active period. (For interpretation of the references to color in this figure legend, the reader is referred to the Web version of this article.)

records from Jeserzersee show that after a clear warming starting at 18.4 ka BP, a marked cold period that lasted from 17.6 cal ka BP to 16.0 cal ka BP ensued. The authors correlate this with the Gschnitz stadial (Schmidt et al., 2012). In comparison with our data, the cooling that culminated between 17.6 and 16.0 ka may have resulted in successively rapid glacier growth and concurrent but possibly slower formation of ice-rich permafrost. Gschnitz stadial glaciers might have soon covered the valley floors in both investigated sites (Tandl and Norbert) down to the moraines we mapped, whereas the surroundings were affected by (discontinuous) permafrost. Although the moraines were not directly dated, the determined ELA lowering of the local Tandl Gschnitz glacier of 800 m is in good agreement with observations from other studies in which Δ ELA of 650–800 m, relative to the LIA, is reported (Gross et al., 1977; Maisch, 1987; Kerschner et al., 1999; Ivy-Ochs et al., 2006a). Summer temperature (JJA) at the ELA during the Gschnitz stadial is estimated to have been around 0.5 °C (Kerschner and Ivy-Ochs, 2008). Using the local modern JJA temperature of 8.7 °C (Auer et al., 2010) determined at around 1880 m a.s.l. (Fig. 6a), a summer temperature lowering of 8.2 °C is obtained. Notably almost the same temperature lowering for the Gschnitz stadial was obtained by Kerschner et al. (1999) in the Gschnitz Valley. In the Seebach Valley (<20 km distance, Fig. 1b), frontal moraines assigned to the Gschnitz stadial are preserved at similar elevation as our moraines, that is between 1000 and 1300 m a.s.l. (Drescher-Schneider and Reitner, 2018).

The exposure ages and cross-cutting relationships of glacier and rockglacier deposits suggest that the Gschnitz stadial glaciers in both valleys receded rapidly and that permafrost development and rockglacier formation started immediately after or even simultaneously with glacier downwasting. It is likely that the oldest rockglaciers (TA complex 1350 m a.s.l. Fig. 3a) evolved from talus that had accumulated during the presence of the Gschnitz stadial glacier, likely along the margins, but was not evacuated by the glacier itself. The Lake Jeserzersee data indicate that after 16.0 ka considerable summer warming occurred, thus markedly before the onset of the Bølling-Allerød Interstadial at 14.7 ka (Schmidt et al., 2012). In both of our study valleys, ice retreat enabled advance of

rockglaciers into the formerly glaciated areas. Schmidt et al. (2012) further infer a shift towards drier conditions at the end of the 17.6–16.0 ka cold phase. This is likely to have strongly favoured rockglacier formation. Talus production was not a limiting factor in the catchment as shown by the deposits of a debris-covered glacier (Norbert Valley) and by the presence of modern talus cones and abundant recent rock fall deposits (Schuster et al., 2006). Debris under permafrost conditions at the margin of the Gschnitz glacier with already interstitial ice, something like an “impeded rockglacier”, might characterize the starting position. Such a setting could explain the limited age difference of only few hundred years observed between the stabilisation of the moraine and that of the relict rockglacier at the Norbert site (Fig. 3b).

During the Bølling-Allerød interstadial, both the Tandl and the Norbert Valleys were likely completely ice-free and open for other (gravitational) processes, e.g. landslides (Tandl Fig. 5a), or development of large talus cones and aprons. In the Tandl area, the landslide deposit and the rockglacier (TC2) on top of it (~2130 m a.s.l.) indicate that the valley was ice-free by the Bølling-Allerød interstadial. This is probably also true for the Norbert site as it is located at similar elevation and even has a southerly aspect. During the warming of the Bølling-Allerød, the permafrost limit shifted to higher elevations (~1600–1800 m a.s.l., Fig. 9) and the rockglaciers that had formed during and towards the end of the Gschnitz stadial stabilised (complex TA, NA, Fig. 3a and b). Nevertheless, it is likely that in both valleys at higher elevation (>1700 m a.s.l.) rockglaciers remained active and even more rockglacier lobes developed (TB, TC and NC).

The Younger Dryas cold period followed and glaciers all across the Alps advanced during the Egesen stadial (Kerschner, 1980; Maisch, 1987; Ivy-Ochs et al., 1996; Kelly et al., 2004; Schindelwig et al., 2012; Moran et al., 2016; Scotti et al., 2017). At the onset of the Younger Dryas, in the study region small cirque glaciers advanced and built up moraines. Such deposits are evidently present at the Tandl site (~2220 m a.s.l.), but are less distinct at the Norbert area. However, it is important to note that there are many large rockglacier deposits of Egesen stadial ages in both valleys at around 1700 m a.s.l., 2290 m a.s.l. and 2330 m a.s.l. (TB1, TC4, NC1).

In Debant Valley (Reitner et al., 2016) and at Kolm Saigurn (Bichler et al., 2016) (Fig. 1b), both about 25 km from our sites, Egesen moraines have been mapped and ^{10}Be dated to around 12 ka. In the latter case even a landslide deposit of Allerød age was overridden. Furthermore, sediments from Lake Stappitzersee (Drescher-Schneider and Reitner, 2018) record both the warming of the Bølling-Allerød and the following climate deterioration of the Younger Dryas. Pollen data from Lake Stappitzersee indicate an abrupt change in terms of temperature lowering but also a drastic reduction in precipitation. Paleo-precipitation calculations of Kerschner et al. (2000) suggest 15–30% less precipitation for the central Eastern Alps during the Younger Dryas. This strongly favours rockglaciers as opposed to glaciers. Our findings clearly support this view both morphologically and geochronologically as documented by the prominent rockglacier deposit TB1 in the Tandl area (1700 m a.s.l.), with stabilisation ages around 12 to 11 ka. The same is true for the Norbert area with stabilisation of NC1 at 11.4 ± 0.5 ka (2330 m a.s.l.). In this region, climatic conditions during the Younger Dryas were ideal for rockglacier development but notably less favourable for glacier advance (cf. Frauenfelder et al. (2001)). Data from other sites indicate that the majority of rock glaciers formed after the maximum glacier extent of the Younger Dryas (Maisch, 1982; Buchenauer, 1990; Sailer and Kerschner, 1999; Lambiel and Reynard, 2000; Ivy-Ochs et al., 2009; Moran et al., 2016). However, our results show that rockglacier and glacier development happened simultaneously, with both topographic (location of the ELA at that time) and climatological factors (including low precipitation sums), playing a key role (cf. Scotti et al. (2013)). Avian and Kellerer-Pirkibauer (2012) modelled the permafrost distribution in the Reisseck mountains during the Younger Dryas based on different temperature scenarios. The permafrost distribution of their coldest scenario, considering a temperature depression of 4°C (relative to LIA temperatures), fits well to the location of our lowest directly dated Egesen rockglacier from the Tandl Valley (TB1) and the calculated MAAT lowering of 5.8°C relative to modern temperature ($\approx 4.4^\circ\text{C}$ relative to LIA).

The last geomorphological evidence of activity linked to permafrost is given with the complex TC1-4 (1890–2290 m a.s.l., Tandl Valley) showing rockglacier final stabilisation in the early Holocene (Figs. 3a and 9). Such a result is surprising as a strong warming trend which occurred at the Lateglacial-Holocene transition proceeded into the early Holocene (Nicolussi et al., 2005; Joerin et al., 2008; Solomina et al., 2015). Dendrochronological evidence shows that around 10 ka the largest Austrian glacier (the Pasterze) was already smaller than today (Nicolussi and Patzelt, 2000) and Holocene glacier size never markedly exceeded that of the LIA (Schimmelpfennig et al., 2014; Le Roy et al., 2015). We suggest that ventilation through the blocky deposits could explain this delay in stabilisation. Numerous studies examined the chimney-effect (Humlum, 1997; Hoelzle et al., 1999; Gude et al., 2003; Sawada et al., 2003; Delaloye and Lambiel, 2005), the impact of air circulation on temperature in blocky deposits, where cold air replaces warm air due to density differences, favouring an overcooling of the deposit. In a recent study in the Malta Valley (Pflüglhof) at an elevation of ~ 900 m a.s.l. and only about 5 km north of the Tandl rockglacier tributary valley (Fig. 1b), Wakonigg (2006) monitored an “unterkühlte Schutthalde” (undercooled talus). Where, even during the exceptional warm years of monitoring (2003–2006), the average summer temperatures of air streaming out at the lower part of the deposit never exceeded $<6.3^\circ\text{C}$, which is much lower than the surrounding landscape with JJA temperatures of 15.3°C (Wakonigg, 2006). The same process can lead to permafrost preservation in well ventilated block fields and rockglaciers several hundreds of meters below the actual

permafrost limit (Juliussen and Humlum, 2008). Considering that the Tandl area had extremely long permafrost-friendly conditions (since the retreat of the Gschnitz glacier), the northern aspect, the low solar radiation, and the very blocky structure which favours the chimney-effect, it seems possible that final stabilisation of the TC rockglacier deposits occurred almost 2 ka after the end of the Younger Dryas cold phase.

6. Conclusions

Our investigation of two outstanding sequences of relict rockglacier deposits in the Reisseck group region using detailed geomorphological field mapping combined with cosmogenic nuclide exposure dating allowed us to unravel the local paleoclimate history and to provide new insights into post-LGM permafrost development. In total 14 rockglacier lobes were exposure dated by analysing 1–6 boulders on each lobe. The determined ages are interpreted as moments of stabilisation.

The exposure ages of the lowest relict rockglaciers of the southwest-facing Norbert site suggest their stabilisation around 15.7 ka at elevations of 1580 m a.s.l. and 1730 m a.s.l., while the lowest relict rockglacier complex at the northeast facing Tandl site at an elevation of 1350 m a.s.l. stabilised around 14 ka. One of the low elevation rockglaciers at the Norbert site is located on top of a debris-covered glacier deposit which we dated to 16 ka. At the Tandl site an ELA depression value of 800 m (1880 m a.s.l.), determined by paleoglacier reconstruction and paleo ELA calculation, agree well with ELA lowering investigated at other Gschnitz stadial glacier localities (Kerschner et al., 1999). Cross-cutting relationships at both study sites of these low elevation rockglacier lobes with glacial deposits allow us to constrain rockglacier formation and thus start of permafrost development immediately after the retreat of the Gschnitz stadial glaciers (~ 16 ka) or nearly simultaneously with retreat. Based on the source areas at the flanks of the Gschnitz glaciers, permafrost most probably already existed during the Gschnitz stadial, which is possibly the first occurrence of permafrost after the retreat of the LGM glaciers in the Eastern Alps. Additionally, the data show that the rockglaciers with a north-eastern aspect stabilised later (~ 1.7 ka) and at lower elevations (by 300–400 m) compared to the rockglaciers with a southwestern aspect. Correlating modern MAAT values at the elevation of these post-Gschnitz rockglacier deposits to an -2°C isotherm results in temperature lowering for the Gschnitz stadial of $5.2\text{--}4.5^\circ\text{C}$ (Norbert, NA1 and NA2) and 6.3°C (Tandl, TA1), respectively. Similarly, from the reconstructed Gschnitz glacier ELA in the Tandl area (1880 m a.s.l.), a lowering of 8.2°C of the summer (JJA) temperature was determined, relative to modern days JJA temperatures.

Upvalley of the post-Gschnitz rockglacier deposits, numerous rockglaciers were observed in both study sites. Obtained exposure ages between 12–10 ka of several rockglacier lobes suggests their stabilisation at the end of the Egesen stadial (11.7 ka). Based on the location of the lowest Tandl Egesen rockglacier lobe (TB1, 1700 m a.s.l.) a MAAT depression of 5.8°C relative to modern temperatures was calculated. Deposits of Egesen glaciers were identified at an elevation of around 2300 m a.s.l., which corresponds well to the known elevation of Egesen stadial glaciers in the area. Glacial deposits are well preserved in the Tandl area but less distinct in the Norbert area. The presence of Egesen stadial glaciers in the study sites and rockglacier deposits that stabilised during the same period indicates their co-existence during the Egesen stadial. The Egesen glacier deposit in the Tandl area overran landslide and rockglacier deposits, which suggests ice-free conditions during the Bølling-Allerød interstadial. Rockglacier formation and thus permafrost development at high elevations >2000 m a.s.l. must have started immediately after the retreat of the Gschnitz glacier

but before the Egesen stadial glacier formed. This observation shows that rockglacier development was possible during the entire Younger Dryas, if the local topography, debris supply, ELA, and associated glacier extent provided the necessary boundary conditions.

This study shows that measuring cosmogenic nuclide concentrations of relict rockglacier deposits, together with geomorphological observations, is a powerful tool for reconstructing local paleoclimate (temperatures) and past permafrost distribution. In contrast to glacial deposits, which are sensitive to degradation through erosion and gravitational processes or post-depositional burial (fans, talus), rockglacier deposits frequently retain a prominent position in the landscape even many thousands of years after activity has ceased.

Credit author statement

Olivia Steinemann: Investigation, Methodology, Writing- Original draft preparation, Visualization; Jürgen M. Reitner: Conceptualization, Investigation, Writing-Review & Editing; Marcus Christl: Formal Analysis, Data Curation, Investigation; Susan Ivy-Ochs: Conceptualization, Methodology, Investigation, Resources, Writing-Review & Editing, Supervision, Funding Acquisition; Hans-Arno Synal: Formal Analysis, Resources.

Data availability

All data generated or analysed during this study are included in the published paper.

Declaration of competing interest

The authors declare that they have no known competing financial interests or personal relationships that could have appeared to influence the work reported in this paper.

Acknowledgements

We thank Isabelle Gärtner-Roer and Ian S. Evans for their careful and thorough reviews of the manuscript. Furthermore, we would like to thank Ueli Steinemann for discussion and support in the field and Hanns Kerschner for inspiring comments on the first version of the manuscript and for help with sampling Tan1 and Tan2. Wilfriede Haslacher-Winter, Ursula Krobath and Hannes Krobath from Winterholz Sägewerk GmbH in Mühldorf, and Günther Baier from the Zundel'sche Forstverwaltung in Malta are thanked for providing us access to the sites. We are grateful for the support of the whole team of the Laboratory of Ion Beam Physics at ETH Zürich, for assistance in the laboratory and the excellent AMS measurements. We thank the Geological Survey of Austria and the province of Carinthia for kindly providing the geological map and the digital elevation model of the area. This work was supported by the Swiss National Science Foundation (SNSF)[175794, 156187].

References

André, M.-F., 2002. Rates of postglacial rock weathering on glacially scoured outcrops (Abisko-Riksgränsen area, 68°N). *Geogr. Ann. Phys. Geogr.* 84 (3/4), 139–150. <https://doi.org/10.1111/j.0435-3676.2002.00168.x>.

Andrés, N., Gómez-Ortiz, A., Fernández-Fernández, J.M., Tanarro, L.M., Salvador-Franch, F., Oliva, M., Palacios, D., 2018. Timing of deglaciation and rock glacier origin in the southeastern Pyrenees: a review and new data. *Boreas* 47 (4), 1050–1071. <https://doi.org/10.1111/bor.12324>.

Arenson, L., Hoelzle, M., Springman, S., 2002. Borehole deformation measurements and internal structure of some rock glaciers in Switzerland. *Permafrost. Periglac. Process.* 13 (2), 117–135. <https://doi.org/10.1002/ppp.414>.

Auer, I., Prettenhaler, F., Böhm, R., Proske, H., 2010. *Zwei Alpentäler im*

Klimawandel. Innsbruck University Press, Innsbruck.

Avian, M., Kellerer-Pirklbauer, A., 2012. Modelling of potential permafrost distribution during the younger Dryas, the Little ice age and at present in the Reisseck mountains, Hohe Tauern range, Austria. *Austrian J. Earth Sci.* 105, 140–153.

Bakke, J., Nesje, A., 2011. Equilibrium-line altitude (ELA). In: Singh, V.P., Singh, P., Haritashya, U.K. (Eds.), *Encyclopedia of Snow, Ice and Glaciers*. Springer, Dordrecht, pp. 268–277. https://doi.org/10.1007/978-90-481-2642-2_140.

Balco, G., Stone, J.O., Lifton, N.A., Dunai, T.J., 2008. A complete and easily accessible means of calculating surface exposure ages or erosion rates from ¹⁰Be and ²⁶Al measurements. *Quat. Geochronol.* 3 (3), 174–195. <https://doi.org/10.1016/j.quageo.2007.12.001>.

Ballantyne, C.K., Schnabel, C., Xu, S., 2009. Exposure dating and reinterpretation of coarse debris accumulations ("rock glaciers") in the Cairngorm Mountains, Scotland. *J. Quat. Sci.* 24 (1), 19–31. <https://doi.org/10.1002/jqs.1189>.

Ballantyne, C.K., 2018. *Periglacial Geomorphology*. Wiley Blackwell, Hoboken.

Barrows, T.T., Stone, J.O., Fifield, L.K., 2004. Exposure ages for Pleistocene periglacial deposits in Australia. *Quat. Sci. Rev.* 23, 697–708. <https://doi.org/10.1016/j.quascirev.2003.10.011>.

Barsch, D., 1992. Permafrost creep and rockglaciers. *Permafrost. Periglac. Process.* 3 (3), 175–188. <https://doi.org/10.1002/ppp.3430030303>.

Barsch, D., 1996. Rockglaciers: Indicators for the Present and Former Geocology in High Mountain Environments. Springer, Berlin. <https://doi.org/10.1007/978-3-642-80093-1>.

Benn, D., Hulton, N., 2010. An Excel spreadsheet program for reconstructing the surface profile of former mountain glaciers and ice caps. *Comput. Geosci.* 36, 605–610. <https://doi.org/10.1016/j.cageo.2009.09.016>.

Bichler, M.G., Reindl, M., Reitner, J.M., Drescher-Schneider, R., Wirsig, C., Christl, M., Hajdas, I., Ivy-Ochs, S., 2016. Landslide deposits as stratigraphical markers for a sequence-based glacial stratigraphy: a case study of a Younger Dryas system in the Eastern Alps. *Boreas* 45 (3), 537–551. <https://doi.org/10.1111/bor.12173>.

Bodin, X., Krysiński, J.M., Schoeneich, P., Le Roux, O., Lorier, L., Echeland, T., Peyron, M., Walpersdorf, A., 2017. The 2006 collapse of the Bérard rock glacier (southern French alps). *Permafrost. Periglac. Process.* 28 (1), 209–223. <https://doi.org/10.1002/ppp.1887>.

Boeckli, L., Brenning, A., Gruber, S., Noetzi, J., 2012a. A statistical approach to modelling permafrost distribution in the European Alps or similar mountain ranges. *Cryosphere* 6 (1), 125–140. <https://doi.org/10.5194/tc-6-125-2012>.

Boeckli, L., Brenning, A., Gruber, S., Noetzi, J., 2012b. Permafrost distribution in the European Alps: calculation and evaluation of an index map and summary statistics. *Cryosphere* 6 (4), 807–820. <https://doi.org/10.5194/tc-6-807-2012>.

Böhlert, R., Compeer, M., Egli, M., Brandová, D., Maisch, M., Kubik, P.W., Haeblerli, W., 2011a. A combination of relative-numerical dating methods indicates two high Alpine rock glacier activity phases after the glacier advance of the Younger Dryas. *Open Geogr. J.* 4 (11), 281–296. <https://doi.org/10.5167/uzh-42941>.

Böhlert, R., Egli, M., Maisch, M., Brandová, D., Ivy-Ochs, S., Kubik, P.W., Haeblerli, W., 2011b. Application of a combination of dating techniques to reconstruct the Lateglacial and early Holocene landscape history of the Albula region (eastern Switzerland). *Geomorphology* 127 (1–2), 1–13. <https://doi.org/10.1016/j.geomorph.2010.10.034>.

Brazier, V., Kirkbride, M.P., Owens, I.F., 1998. The relationship between climate and rock glacier distribution in the Ben Ohau Range, New Zealand. *Geogr. Ann. Phys. Geogr.* 80, 193–207.

Buchenaue, H.W., 1990. *Gletscher-und Blockgletschergeschichte der westlichen Schobergruppe (Osttirol)*. Marburg/Lahn: Marburger Geographische Gesellschaft.

Capps, S.R., 1910. Rock glaciers in Alaska. *J. Geol.* 18 (4), 359–375.

Christl, M., Vockenhuber, C., Kubik, P.W., Wacker, L., Lachner, J., Alfmov, V., Synal, H.A., 2013. The ETH Zurich AMS facilities: performance parameters and reference materials. *Nucl. Instrum. Methods Phys. Res. Sect. B Beam Interact. Mater. Atoms* 294, 29–38. <https://doi.org/10.1016/j.nimb.2012.03.004>.

Claude, A., Ivy-Ochs, S., Kober, F., Antognini, M., Salcher, B., Kubik, P.W., 2014. The Chironico landslide (Valle Leventina, southern Swiss Alps): age and evolution. *Swiss J. Geosci.* 107 (2–3), 273–291. <https://doi.org/10.1007/s00015-014-0170-z>.

Cossart, E., Fort, M., Bourlès, D., Braucher, R., Perrier, R., Siame, L., 2012. Deglaciation pattern during the Lateglacial/Holocene transition in the southern French Alps. Chronological data and geographical reconstruction from the Clarée Valley (upper Durance catchment, southeastern France). *Palaeogeogr. Palaeoclimatol. Palaeoecol.* 315–316, 109–123. <https://doi.org/10.1016/j.palaeo.2011.11.017>.

Delaloye, R., Lambiel, C., 2005. Evidence of winter ascending air circulation throughout talus slopes and rock glaciers situated in the lower belt of alpine discontinuous permafrost (Swiss Alps). *Norsk Geografisk Tidsskrift - Norwegian J. Geogr.* 59 (2), 194–203. <https://doi.org/10.1080/00291950510020673>.

Delaloye, R., Lambiel, C., Gärtner-Roer, I., 2010. Overview of rock glacier kinematics research in the Swiss Alps. *Geograph. Helv.* 65 (2), 135–145. <https://doi.org/10.5194/gh-65-135-2010>.

Delaloye, R., Morard, S., Barboux, C., Abbet, D., Gruber, V., Riedo, M., Gachet, S., 2013. Rapidly moving rock glaciers in Matternal. *Matternal—ein Tal in Bewegung*. In: Graf, C. (Ed.), *Publikation zur Jahrestagung der Schweizerischen Geomorphologischen Gesellschaft*, vol. 29, pp. 21–31.

Delunel, R., Bourlès, D.L., van der Beek, P.A., Schlunegger, F., Leya, I., Masarik, J., Paquet, E., 2014. Snow shielding factors for cosmogenic nuclide dating inferred from long-term neutron detector monitoring. *Quat. Geochronol.* 24, 16–26. <https://doi.org/10.1016/j.quageo.2014.07.003>.

Dramis, F., Giraudi, C., Guglielmin, M., 2003. Rock glacier distribution and paleoclimate in Italy. *Permafrost* 1, 199–204.

- Drescher-Schneider, R., Reitner, J., 2018. Die Neuinterpretation der Stappitzer See-Bohrungen im Kontext der Klimageschichte und Landschaftsentwicklung. *Carinth. II* 208 (128), 369–398.
- Ehlers, J., Gibbard, P.L., 2004. Quaternary Glaciations-Extent and Chronology: Part I: Europe. Elsevier, Amsterdam.
- Ehlers, J., Gibbard, P.L., Hughes, P.D., 2011. Quaternary Glaciations-Extent and Chronology: a Closer Look. Elsevier, Amsterdam.
- Eriksen, H.Ø., Rouyet, L., Lauknes, T.R., Berthling, I., Isaksen, K., Hindberg, H., Larsen, Y., Corner, G.D., 2018. Recent acceleration of a rock glacier complex, Ådjet, Norway, documented by 62 years of remote sensing observations. *Geophys. Res. Lett.* 45 (16), 8314–8323. <https://doi.org/10.1029/2018GL077605>.
- Frauenfelder, R., Kääb, A., 2000. Towards a palaeoclimatic model of rock-glacier formation in the Swiss Alps. *Ann. Glaciol.* 31 (1), 281–286.
- Frauenfelder, R., Haeblerli, W., Hoelzle, M., Maisch, M., 2001. Using relict rockglaciers in GIS-based modelling to reconstruct Younger Dryas permafrost distribution patterns in the Err-Julier area, Swiss Alp. *Norsk Geografisk Tidsskrift-Norwegian J. Geogr.* 55 (4), 195–202.
- Frauenfelder, R., 2003. Rockglacier occurrence and related terrain parameters in a study area of the eastern Swiss alps. In: 8th International Conference on Permafrost, pp. 253–258.
- Frauenfelder, R., Laustela, M., Kääb, A., 2004. Velocities and relative surface ages of selected Alpine rockglaciers. *Mitteilungen der Versuchsanstalt für Wasserbau, Hydrologie und Glaziologie an der Eidgenössischen Technischen Hochschule Zurich* (184), 103–118.
- Frehner, M., Ling, A.H.M., Gärtner-Roer, I., 2015. Furrow-and-ridge morphology on rockglaciers explained by gravity-driven buckle folding: a case study from the Murtèl rockglacier (Switzerland). *Permafrost: Periglac. Process.* 26 (1), 57–66. <https://doi.org/10.1002/ppp.1831>.
- Fuchs, M.C., Böhlert, R., Krbetschek, M., Preusser, F., Egli, M., 2013. Exploring the potential of luminescence methods for dating Alpine rock glaciers. *Quat. Geochronol.* 18, 17–33. <https://doi.org/10.1016/j.quageo.2013.07.001>.
- González Trueba, J.J., Serrano Cañadas, E., 2004. El método AAR para la determinación de Paleo-ELAs: análisis metodológico y aplicación en el macizo de Valdecebollas (Cordillera Cantábrica). *Cuadernos de investigación geográfica/Geogr. Res. Lett.* 30, 7–34.
- Grischott, R., Kober, F., Lupker, M., Reitner, J.M., Drescher-Schneider, R., Hajdas, I., Christl, M., Willett, S.D., 2017. Millennial scale variability of denudation rates for the last 15 kyr inferred from the detrital ^{10}Be record of Lake Stappitz in the Hohe Tauern massif, Austrian Alps. *Holocene* 27 (12), 1914–1927. <https://doi.org/10.1177/0959683617708451>.
- Gross, G., Kerschner, H., Patzelt, G., 1977. Methodische Untersuchungen über die Schneegrenze in alpinen Gletschergebieten. *Z. Gletscherkd. Glazialgeol.* 12, 223–251.
- Gross, G., Patzelt, G., 2015. The Austrian Glacier Inventory for the Little Ice Age Maximum (GI LIA) in ArcGIS (shapefile) format. PANGAEA - Data Publisher for Earth & Environmental Science. <https://doi.org/10.1594/PANGAEA.844987>.
- Gruber, S., Hoelzle, M., 2001. Statistical modelling of mountain permafrost distribution: local calibration and incorporation of remotely sensed data. *Permafrost: Periglac. Process.* 12 (1), 69–77. <https://doi.org/10.1002/ppp.374>.
- Gude, M., Dietrich, S., Maeusbacher, R., Hauck, C., Molenda, R., Ruzicka, V., Zacharda, M., 2003. Probable Occurrence of Sporadic Permafrost in Non-alpine Scree Slopes in Central Europe. 8th International Conference on Permafrost, Zurich, Switzerland, pp. 331–336.
- Haeblerli, W., 1985. Creep of mountain permafrost. *Mitteilungen der Versuchsanstalt für Wasserbau, Hydrologie und Glaziologie der ETH Zürich* 77, 142.
- Haeblerli, W., Hoelzle, M., Kääb, A., Keller, F., Vonder Mühl, D., Wagner, S., 1998. Ten years after drilling through the permafrost of the active rock glacier Murtèl, Eastern Swiss Alps: answered questions and new perspectives. In: Proceedings of the 7th International Conference on Permafrost, pp. 403–410.
- Haeblerli, W., Kääb, A., Wagner, S., Vonder Mühl, D., Geissler, P., Haas, J.N., Glatzel-Mattheier, H., Wagenbach, D., 1999. Pollen analysis and ^{14}C age of moss remains in a permafrost core recovered from the active rock glacier Murtèl-Corvatsch, Swiss Alps: geomorphological and glaciological implications. *J. Glaciol.* 45 (149), 1–8. <https://doi.org/10.1017/S0022143000002975>.
- Haeblerli, W., Brandova, D., Burga, C., Egli, M., Frauenfelder, R., Kääb, A., Maisch, M., Mauz, B., Dikau, R., 2003. Methods for absolute and relative age dating of rock-glacier surfaces in alpine permafrost. Proceedings of the 8th International Conference on Permafrost, Zurich, Switzerland, pp. 343–348.
- Haeblerli, W., Hallet, B., Arenson, L., Elconin, R., Humlum, O., Kääb, A., Kaufmann, V., Ladanyi, B., Matsuoka, N., Springman, S., Mühl, D.V., 2006. Permafrost creep and rock glacier dynamics. *Permafrost: Periglac. Process.* 17, 189–214. <https://doi.org/10.1002/ppp.561>.
- Hedding, D., 2011. Pronival rampart and protalus rampart: a review of terminology. *J. Glaciol.* 57 (206), 1179–1180. <https://doi.org/10.3189/002214311798843241>.
- Heiri, O., Koinig, K.A., Spötl, C., Barrett, S., Brauer, A., Drescher-Schneider, R., Gaar, D., Ivy-Ochs, S., Kerschner, H., Luetscher, M., 2014. Palaeoclimate records 60–8 ka in the Austrian and Swiss Alps and their forelands. *Quat. Sci. Rev.* 106, 186–205. <https://doi.org/10.1016/j.quascirev.2014.05.021>.
- Hippolyte, J.-C., Bourlès, D., Braucher, R., Carcaillet, J., Léanni, L., Arnold, M., Aumaitre, G., 2009. Cosmogenic ^{10}Be dating of a sacking and its faulted rock glaciers, in the Alps of Savoy (France). *Geomorphology* 108 (3), 312–320. <https://doi.org/10.1016/j.geomorph.2009.02.024>.
- Hoelzle, M., Wagner, S., Kääb, A., Vonder Mühl, D., 1998. Surface movement and internal deformation of ice-rock mixtures within rock glaciers at Pontresina-Schafberg, Upper Engadin, Switzerland. In: 7th International Conference on Permafrost. Canada, Quebec, pp. 465–471.
- Hoelzle, M., Wegmann, M., Krummenacher, B., 1999. Miniature temperature data-loggers for mapping and monitoring of permafrost in high mountain areas: first experience from the Swiss Alps. *Permafrost: Periglac. Process.* 10 (2), 113–124. [https://doi.org/10.1002/\(SICI\)1099-1530\(199904\)06<10:23.O.CO;2-A](https://doi.org/10.1002/(SICI)1099-1530(199904)06<10:23.O.CO;2-A).
- Huber, K., Weckström, K., Drescher-Schneider, R., Knoll, J., Schmidt, J., Schmidt, R., 2010. Climate changes during the last glacial termination inferred from diatom-based temperatures and pollen in a sediment core from Längsee (Austria). *J. Paleolimnol.* 43 (1), 131. <https://doi.org/10.1007/s10933-009-9322-y>.
- Humlum, O., 1997. Active layer thermal regime at three rock glaciers in Greenland. *Permafrost: Periglac. Process.* 8 (4), 383–408. [https://doi.org/10.1002/\(sici\)1099-1530\(199710\)12<4:383::aid-ppp265>3.3.co;2-m](https://doi.org/10.1002/(sici)1099-1530(199710)12<4:383::aid-ppp265>3.3.co;2-m).
- Ikedda, N., Matsuoka, N., 2002. Degradation of talus-derived rock glaciers in the Upper Engadin, Swiss Alps. *Permafrost: Periglac. Process.* 13 (2), 145–161. <https://doi.org/10.1002/ppp.413>.
- Ivy-Ochs, S., Schlichter, C., Kubik, P., Beer, J., Kerschner, H., 1996. The exposure age of an Egesen moraine at Julier Pass measured with the cosmogenic radionuclides ^{10}Be , ^{26}Al and ^{36}Cl . *Eclogae Geol. Helv.* 89, 1049–1063.
- Ivy-Ochs, S., Kerschner, H., Kubik, P.W., Schlichter, C., 2006a. Glacier response in the European alps to Heinrich event 1 cooling: the Gschnitz stadial. *J. Quat. Sci.* 21 (2), 115–130. <https://doi.org/10.1002/jqs.955>.
- Ivy-Ochs, S., Kerschner, H., Reuther, A., Maisch, M., Sailer, R., Schaefer, J., Kubik, P., Synal, A., Schlichter, C., 2006b. The In: Timing of Glacier Advances in the Northern European Alps Based on Surface Exposure Dating with Cosmogenic ^{10}Be , ^{26}Al , ^{36}Cl and ^{21}Ne , vol. 415. Geological Society of America Special Paper, pp. 43–60. [https://doi.org/10.1130/2006.2415\(04](https://doi.org/10.1130/2006.2415(04)
- Ivy-Ochs, S., Kerschner, H., Maisch, M., Christl, M., Kubik, P.W., Schlichter, C., 2009. Latest pleistocene and Holocene glacier variations in the European alps. *Quat. Sci. Rev.* 28, 2137–2149. <https://doi.org/10.1016/j.quascirev.2009.03.009>.
- Ivy-Ochs, S., 2015. Glacier variations in the European Alps at the end of the last glaciation. *Cuadernos de Investigación Geográfica* 41 (2), 295–315.
- Joerin, U.E., Nicolussi, K., Fischer, A., Stocker, T.F., Schlichter, C., 2008. Holocene optimum events inferred from subglacial sediments at Tschierwa Glacier, Eastern Swiss Alps. *Quat. Sci. Rev.* 27 (3–4), 337–350. <https://doi.org/10.1016/j.quascirev.2007.10.016>.
- Johnson, B.G., Thackray, G.D., Van Kirk, R., 2007. The effect of topography, latitude, and lithology on rock glacier distribution in the Lemhi Range, central Idaho, USA. *Geomorphology* 91 (1), 38–50. <https://doi.org/10.1016/j.geomorph.2007.01.023>.
- Jones, D.B., Harrison, S., Anderson, K., Whalley, W.B., 2019. Rock glaciers and mountain hydrology: a review. *Earth Sci. Rev.* 193, 66–90. <https://doi.org/10.1016/j.earscirev.2019.04.001>.
- Juliussen, H., Humlum, O., 2008. Thermal regime of openwork block fields on the mountains Elgähogna and Solen, central-eastern Norway. *Permafrost: Periglac. Process.* 19 (1), 1–18. <https://doi.org/10.1002/ppp.607>.
- Kääb, A., Kaufmann, V., Ladstädter, R., Eiken, T., 2003. Rock Glacier Dynamics: Implications from High-Resolution Measurements of Surface Velocity Fields. 8th International Conference on Permafrost, pp. 501–506.
- Kääb, A., Frauenfelder, R., Roer, I., 2007. On the response of rockglacier creep to surface temperature increase. *Global Planet. Change* 56 (1), 172–187. <https://doi.org/10.1016/j.gloplacha.2006.07.005>.
- Kääb, A., 2013. Rock glaciers and protalus forms. In: Elias, S.A., Mock, C.J. (Eds.), *Encyclopedia of Quaternary Science*, second ed. Elsevier, Amsterdam, pp. 535–541. <https://doi.org/10.1016/B978-0-444-53643-3.00104-7>.
- Kellerer-Pirklbauer, A., Kaufmann, V., 2012. About the relationship between rock glacier velocity and climate parameters in central Austria. *Austrian J. Earth Sci.* 105 (2), 94–112.
- Kellerer-Pirklbauer, A., Lieb, G.K., Kleinfelchner, H., 2012. A new rock glacier inventory of the Eastern European Alps. *Austrian J. Earth Sci.* 105, 78–93.
- Kellerer Pirklbauer, A., Kaufmann, V., 2018. Deglaciation and its impact on permafrost and rock glacier evolution: new insight from two adjacent cirques in Austria. *Sci. Total Environ.* 621, 1397–1414. <https://doi.org/10.1016/j.scitotenv.2017.10.087>.
- Kelly, M.A., Kubik, P.W., Von Blanckenburg, F., Schlichter, C., 2004. Surface exposure dating of the Great Aletsch Glacier Egesen moraine system, western Swiss Alps, using the cosmogenic nuclide ^{10}Be . *J. Quat. Sci.* 19 (5), 431–441. <https://doi.org/10.1002/jqs.854>.
- Kenner, R., Magnusson, J., 2017. Estimating the effect of different influencing factors on rock glacier development in two regions in the Swiss alps. *Permafrost: Periglac. Process.* 28 (1), 195–208. <https://doi.org/10.1002/ppp.1910>.
- Kerschner, H., 1978. Paleoclimatic inferences from Late Würm rock glaciers, eastern central Alps, western Tyrol, Austria. *Arct. Alp. Res.* 10 (3), 635–644. <https://doi.org/10.2307/1550684>.
- Kerschner, H., 1980. Outlines of the climate during the Egesen advance (younger Dryas, 11000–10 000 BP) in the central alps of the western Tyrol, Austria. *Z. Gletscherkd. Glazialgeol.* 16 (2), 229–240.
- Kerschner, H., 1983. Lateglacial Paleotemperatures and Paleoprecipitation as Derived from Permafrost:glacier Relationships in the Tyrolean Alps, Austria. Fourth International Conference on Permafrost, Washington D.C., pp. 589–594.
- Kerschner, H., 1985. Quantitative palaeoclimatic inferences from late glacial snowline, timberline and rock glacier data, Tyrolean Alps, Austria. *Z. Gletscherkd. Glazialgeol.* 21, 363–369.
- Kerschner, H., Ivy-Ochs, S., Schlichter, C., 1999. Paleoclimatic interpretation of the early Late-glacial glacier in the Gschnitz valley, central Alps, Austria. *Ann. Glaciol.* 28 (1), 135–140. <https://doi.org/10.3189/172756499781821661>.

- Kerschner, H., Kaser, G., Sailer, R., 2000. Alpine Younger Dryas glaciers as palaeo-precipitation gauges. *Ann. Glaciol.* 31, 80–84. <https://doi.org/10.3189/172756400781820237>.
- Kerschner, H., Ivy-Ochs, S., 2008. Palaeoclimate from glaciers: examples from the eastern alps during the alpine lateglacial and early Holocene. *Global Planet. Change* 60, 58–71. <https://doi.org/10.1016/j.gloplacha.2006.07.034>.
- Knight, J., Harrison, S., Jones, D.B., 2019. Rock glaciers and the geomorphological evolution of deglaciating mountains. *Geomorphology* 324, 14–24. <https://doi.org/10.1016/j.geomorph.2018.09.020>.
- Kohl, C.P., Nishiizumi, K., 1992. Chemical isolation of quartz for measurement of in-situ produced cosmogenic nuclides. *Geochem. Cosmochim. Acta* 56 (9), 3583–3587.
- Krainer, K., Bressan, D., Dietre, B., Haas, J.N., Hajdas, I., Lang, K., Mair, V., Nickus, U., Reidl, D., Thies, H., 2015. A 10,300-year-old permafrost core from the active rock glacier Lazaun, southern Ötztal Alps (South Tyrol, northern Italy). *Quat. Res.* 83 (2), 324–335. <https://doi.org/10.1016/j.qures.2014.12.005>.
- Lal, D., 1991. Cosmic ray labeling of erosion surfaces: in situ nuclide production rates and erosion models. *Earth Planet. Sci. Lett.* 104, 424–439. [https://doi.org/10.1016/0012-821X\(91\)90220-C](https://doi.org/10.1016/0012-821X(91)90220-C).
- Lambiel, C., Reynard, E., 2000. Cartographie de la distribution du pergélisol et datation des glaciers rocheux dans la région du Mont Gelé (Valais). *Entwicklungsstendenzen und Zukunftsperspektiven in der Geomorphologie. Physische Geographie*. Zürich 41, 91–104.
- Le Roy, M., Nicolussi, K., Deline, P., Astrade, L., Edouard, J.L., Miramont, C., Arnaud, F., 2015. Calendar-dated glacier variations in the western European alps during the neoglacial: the mer de Glace record, mont Blanc massif. *Quat. Sci. Rev.* 108, 1–22. <https://doi.org/10.1016/j.quascirev.2014.10.033>.
- Lieb, G.K., 1993. Zur quantitativen Erfassung des Rückgangs der Kärntner Gletscher vom Hochstand um 1850 bis 1969. Arbeiten aus dem Institut für Geographie der Universitaet Graz 31, 231–251.
- Maisch, M., 1982. Zur Gletscher- und Klimageschichte des alpinen Spätglazials. *Geograph. Helv.* 37, 93–104. <https://doi.org/10.5169/seals-58303>.
- Maisch, M., 1987. Zur Gletscher-, Vegetations- und Klimageschichte der Schweiz seit der Späteiszeit. *Geograph. Helv.* 42, 63–91. <https://doi.org/10.5169/seals-62182>.
- Mattson, L.E., Gardner, J.S., Young, G.J., 1993. Ablation on Debris Covered Glaciers: an Example from the Rakhiot Glacier, Punjab, Himalaya. *Snow and glacier hydrology*, Kathmandu, pp. 289–296.
- Menzies, J., Reitner, J.M., 2016. Microsedimentology of ice stream tills from the Eastern Alps, Austria – a new perspective on till microstructures. *Boreas* 45 (4), 804–827. <https://doi.org/10.1111/bor.12189>.
- Merz, K., Maurer, H., Rabenstein, L., Buchli, T., Springman, S.M., Zweifel, M., 2015. Multidisciplinary geophysical investigations over an alpine rock glacier. *Geophysics* 81 (1), 147–157. <https://doi.org/10.1190/GEO2015-0157.1>.
- Messerli, A., Grinsted, A., 2015. Image georectification and feature tracking toolbox: ImGRAFT. *Geosci. Instrum. Methods Data Syst.* 4 (1), 23–34. <https://doi.org/10.5194/gi-4-23-2015>.
- Monegato, G., Scardia, G., Hajdas, I., Rizzini, F., Piccin, A., 2017. The Alpine LGM in the boreal ice-sheets game. *Sci. Rep.* <https://doi.org/10.1038/s41598-017-02148-7>.
- Moran, A.P., Ivy-Ochs, S., Vockenhuber, C., Kerschner, H., 2016. rock glacier development in the northern calcareous alps at the pleistocene-Holocene boundary. *Geomorphology* 273, 178–188. <https://doi.org/10.1016/j.geomorph.2016.08.017>.
- Nicolussi, K., Patzelt, G., 2000. Discovery of early Holocene wood and peat on the forefield of the Pasterze glacier, eastern alps, Austria. *Holocene* 10 (2), 191–199. <https://doi.org/10.1191/0959683006685842>.
- Nicolussi, K., Kaufmann, M., Patzelt, G., Plicht van der, J., Thurner, A., 2005. Holocene tree-line variability in the Kauner Valley, Central Eastern Alps, indicated by dendrochronological analysis of living trees and subfossil logs. *Veg. Hist. Archaeobotany* 14 (3), 221–234. <https://doi.org/10.1007/s00334-005-0013-y>.
- Nishiizumi, K., Imamura, M., Caffee, M.W., Southon, J.R., Finkel, R.C., McAninch, J., 2007. Absolute calibration of ¹⁰Be AMS standards. *Nucl. Instrum. Methods Phys. Res. Sect. B Beam Interact. Mater. Atoms* 258 (2), 403–413. <https://doi.org/10.1016/j.nimb.2007.01.297>.
- Noetzi, J., Gruber, S., Kohl, T., Salzmann, N., Haeblerli, W., 2007. Three-dimensional distribution and evolution of permafrost temperatures in idealized high-mountain topography. *J. Geophys. Res.* 112 (F02S13) <https://doi.org/10.1029/2006JF000545>.
- Ohmura, A., Kasser, P., Funk, M., 1992. Climate at the equilibrium line of glaciers. *J. Glaciol.* 38 (130), 397–411. <https://doi.org/10.3189/S0022143000002276>.
- Palacios, D., Gómez-Ortiz, A., Andrés, N., Salvador, F., Oliva, M., 2016. Timing and new geomorphologic evidence of the last deglaciation stages in Sierra Nevada (southern Spain). *Quat. Sci. Rev.* 150, 110–129. <https://doi.org/10.1016/j.quascirev.2016.08.012>.
- Pellitero, R., Rea, B.R., Spagnolo, M., Bakke, J., Hughes, P., Ivy-Ochs, S., Lukas, S., Ribolini, A., 2015. A GIS tool for automatic calculation of glacier equilibrium-line altitudes. *Comput. Geosci.* 82, 55–62. <https://doi.org/10.1016/j.cageo.2015.05.005>.
- Pellitero, R., Rea, B.R., Spagnolo, M., Bakke, J., Ivy-Ochs, S., Frew, C.R., Hughes, P., Ribolini, A., Lukas, S., Renssen, H., 2016. Glare, a GIS tool to reconstruct the 3D surface of palaeoglaciers. *Comput. Geosci.* 94, 77–85. <https://doi.org/10.1016/j.cageo.2016.06.008>.
- Pestal, G., Rataj, W., Reitner, J.M., Schuster, R., 2006. Österreichische Geologische Karte 1:50.000 Bl. 182, Spittal an der Drau. Geologische Bundesanstalt, Wien.
- Pratap, B., Dobhal, D., Mehta, M., Bhambri, R., 2014. Influence of debris cover and altitude on glacier surface melting: a case study on Dokriani Glacier, central Himalaya, India. *Ann. Glaciol.* 56 (70), 9–16. <https://doi.org/10.3189/2015AoG70A971>.
- Reitner, J.M., 2007a. Glacial dynamics at the beginning of Termination I in the Eastern Alps and their stratigraphic implications. *Quat. Int.* 164–165, 64–84.
- Reitner, J.M., 2007b. Bericht 2005–2006 über geologische Aufnahmen im Quartär auf Blatt 182 Spittal an der Drau. *Jahrb. Geol. Bundesanst. Wien* 147 (3–4), 672–676.
- Reitner, J.M., Ivy-Ochs, S., Drescher-Schneider, R., Hajda, I., Linner, M., 2016. Reconsidering the current stratigraphy of the Alpine Lateglacial: implications of the sedimentary and morphological record of the Lienz area (Tyrol/Austria). *Quat. Sci. J.* 65 (2), 144. <https://doi.org/10.3285/eg.65.2.02>.
- Roer, I., Käab, A., Dikau, R., 2005. Rockglacier acceleration in the Turtmann valley (Swiss alps): probable controls. *Norsk Geografisk Tidsskrift - Norwegian J. Geogr.* 59 (2), 157–163. <https://doi.org/10.1080/00291950510020655>.
- Sailer, R., Kerschner, H., 1999. Equilibrium-line altitudes and rock glaciers during the Younger Dryas cooling event, Ferwall group, western Tyrol, Austria. *Ann. Glaciol.* 28 (1), 141–145. <https://doi.org/10.3189/172756499781821698>.
- Sawada, Y., Ishikawa, M., Ono, Y., 2003. Thermal regime of sporadic permafrost in a block slope on Mt. Nishi-Nupukaishinupuri, Hokkaido Island, northern Japan. *Geomorphology* 52 (1), 121–130. [https://doi.org/10.1016/S0169-555X\(02\)00252-0](https://doi.org/10.1016/S0169-555X(02)00252-0).
- Scapozza, C., Lambiel, C., Reynard, E., Fallot, J.-M., Antognini, M., Schoeneich, P., 2010. Radiocarbon dating of fossil wood remains buried by the Piancabella rock glacier, Blenio Valley (Ticino, southern Swiss Alps): implications for rock glacier, treeline and climate history. *Permafrost. Periglac. Process.* 21, 90–96. <https://doi.org/10.1002/ppp.673>.
- Scapozza, C., 2015. Evolution des glaciers et du pergélisol depuis le dernier maximum glaciaire dans la région du mont gelemont fort (Alpes Valaisannes, Suisse) chronologie, modalités de la dernière deglaciation et datations des ages d'exposition a l'aide du Marteau de Schmidt. *Quaternaire* 26 (2), 141–173. <https://doi.org/10.4000/quaternaire.7250>.
- Schimmelpfennig, I., Schaefer, J.M., Akçar, N., Koffman, T., Ivy-Ochs, S., Schwartz, R., Finkel, R.C., Zimmerman, S., Schlüchter, C., 2014. A chronology of Holocene and Little Ice Age glacier culminations of the Steingletscher, Central Alps, Switzerland, based on high-sensitivity beryllium-10 moraine dating. *Earth Planet. Sci. Lett.* 393, 220–230. <https://doi.org/10.1016/j.epsl.2014.02.046>.
- Schindelwig, I., Akçar, N., Kubik, P.W., Schlüchter, C., 2012. Lateglacial and early Holocene dynamics of adjacent valley glaciers in the Western Swiss Alps. *J. Quat. Sci.* 27 (1), 114–124. <https://doi.org/10.1002/jqs.1523>.
- Schmidt, R., Wunsam, S., Brosch, U., Fott, J., Lami, A., Löffler, H., Marchetto, A., Müller, H.W., Pražáková, M., Schwaighofer, B., 1998. Late and post-glacial history of meromictic Längsee (Austria), in respect to climate change and anthropogenic impact. *Aquat. Sci.* 60 (1), 56–88. <https://doi.org/10.1007/PL00001313>.
- Schmidt, R., Weckström, K., Lauterbach, S., Tessadri, R., Huber, K., 2012. North Atlantic climate impact on early late-glacial climate oscillations in the south-eastern Alps inferred from a multi-proxy lake sediment record. *J. Quat. Sci.* 27 (1), 40–50. <https://doi.org/10.1002/jqs.1505>.
- Scotti, R., Brardinoni, F., Alberti, S., Frattini, P., Crosta, G.B., 2013. A regional inventory of rock glaciers and proglacial ramparts in the central Italian Alps. *Geomorphology* 186, 136–149. <https://doi.org/10.1016/j.geomorph.2012.12.028>.
- Scotti, R., Brardinoni, F., Crosta, G.B., Cola, G., Mair, V., 2017. Time constraints for post-LGM landscape response to deglaciation in Val Viola, Central Italian Alps. *Quat. Sci. Rev.* 177, 10–33. <https://doi.org/10.1016/j.quascirev.2017.10.011>.
- Schuster, R., Pestal, G., Reitner, J.M., 2006. Erläuterungen zu Blatt 182 Spittal an der Drau. Geologische Bundesanstalt, Vienna.
- Scotti, R., Brardinoni, F., 2018. Evaluating millennial to contemporary time scales of glacier change in Val Viola, Central Italian Alps. *Geogr. Ann. Phys. Geogr.* 100 (4), 319–339. <https://doi.org/10.1080/104353676.2018.1491312>.
- Solomina, O.N., Bradley, R.S., Hodgson, D.A., Ivy-Ochs, S., Jomelli, V., Mackintosh, A.N., Nesje, A., Owen, L.A., Wanner, H., Wiles, G.C., Young, N.E., 2015. Holocene glacier fluctuations. *Quat. Sci. Rev.* 111, 9–34. <https://doi.org/10.1016/j.quascirev.2014.11.018>.
- Springman, S.M., Arenson, L.U., Yamamoto, Y., Maurer, H., Kos, A., Buchli, T., Derungs, G., 2012. Multidisciplinary investigations on three rock glaciers in the Swiss Alps: legacies and future perspectives. *Geogr. Ann. Phys. Geogr.* 94 (2), 215–243. <https://doi.org/10.1111/j.1468-0459.2012.00464.x>.
- Stone, J.O., 2000. Air pressure and cosmogenic isotope production. *J. Geophys. Res.: Solid Earth* 105 (B10), 23753–23759. <https://doi.org/10.1029/2000JB900181>.
- Van Husen, D., 1987. Die Ostalpen in den Eiszeiten, Aus der geologischen Geschichte Österreichs. Verlag der geologischen Bundesanstalt, Wien.
- Wakonigg, H., 2006. Die unterkühlte Blockschutthalde beim Pflüghof im Maltatal: Ergebnisse von Temperatur-Dauerregistrierungen von April 2001 bis Mai 2004. *Carinth. II* 96 (116), 501–518.
- Walker, M.J.C., Björck, S., Lowe, J.J., Cwynar, L.C., Johnsen, S., Knudsen, K.L., Wohlfarth, B., 1999. Isotopic 'events' in the GRIP ice core: a stratotype for the Late Pleistocene. *Quat. Sci. Rev.* 18 (10–11), 1143–1150. [https://doi.org/10.1016/S0277-3791\(99\)00023-2](https://doi.org/10.1016/S0277-3791(99)00023-2).
- Winkler, S., Lambiel, C., 2018. Age constraints of rock glaciers in the Southern Alps/ New Zealand – exploring their palaeoclimatic potential. *Holocene* 28 (5), 778–790. <https://doi.org/10.1177/0959683618756802>.
- Wirsig, C., Zasadini, J., Ivy-Ochs, S., Christl, M., Kober, F., Schlüchter, C., 2016. A deglaciation model of the Oberhasli, Switzerland. *J. Quat. Sci.* 31 (1), 46–59. <https://doi.org/10.1002/jqs.2831>.
- Wirsig, C., Ivy-Ochs, S., Reitner, J.M., Christl, M., Vockenhuber, C., Bichler, M., Reindl, M., 2017. Subglacial abrasion rates at Goldbergkees, Hohe Tauern, Austria, determined from cosmogenic ¹⁰Be and ³⁶Cl concentrations. *Earth Surf. Process. Landforms* 42 (7), 1119–1131. <https://doi.org/10.1002/esp.4093>.